

Randomized Quaternion UTV Decomposition and Randomized Quaternion Tensor UTV Decomposition

Liqiao Yang^a, Jifei Miao^b, Yanlin Zhang^c, Kit Ian Kou^{c,*}

^a*School of Computing and Artificial Intelligence, Southwestern University of Finance and Economics, Chengdu, Sichuan, 611130, China*

^b*School of Mathematics and Statistics, Yunnan University, Kunming, Yunnan, 650091, China*

^c*Department of Mathematics, Faculty of Science and Technology, University of Macau, Macau 999078, China*

Abstract

In this paper, the quaternion matrix UTV (QUTV) decomposition and quaternion tensor UTV (QTUTV) decomposition are proposed. To begin, the terms QUTV and QTUTV are defined, followed by the algorithms. Subsequently, by employing random sampling from the quaternion normal distribution, randomized QUTV and randomized QTUTV are generated to provide enhanced algorithmic efficiency. Furthermore, theoretical analysis is discussed. Specifically, upper bounds for approximating QUTV and QTUTV are provided, followed by deterministic error bounds and average-case error bounds for the randomized situations. Finally, numerous numerical experiments are presented to verify that the proposed algorithms work more efficiently and with similar relative errors compared to other comparable decomposition methods. This indicates that they could be used in computer vision and other related fields.

Keywords: Quaternion UTV, Randomized algorithm, Quaternion tensor, Deterministic error.

*Corresponding author

Email addresses: liqiaoyoung@163.com (Liqiao Yang), jifmiao@163.com (Jifei Miao), yanlnzhang@163.com (Yanlin Zhang), kikou@umac.mo (Kit Ian Kou)

1. Introduction

As the concept of quaternion is proposed by Hamilton in 1843 [1], quaternions and quaternion matrices are gradually applied to various fields. Such as Bayro *et al.* pioneered in the application of quaternion to robotics [2, 3] and neurocomputing [4], etc. Besides, computer vision based on quaternion representation also has received widespread attention, such as image restoration [5], face recognition [6], and watermarking [7], etc. For the approaches based on quaternion representation, a vital problem is to find a cost-saving expression. Since many data matrices are low-rank inherently, there are various approaches to get the low-rank expression to approximate the original data.

For quaternion matrix, one of the most direct method is to optimize the description of low rankness for the target quaternion matrix basing on Quaternion Singular Value Decomposition (QSVD). Similar to the real cases, the rank of quaternion matrix is defined as the number of non-zero singular values, and the quaternion nuclear norm (QNN) as an efficient replacement of rank has been well researched. In specific, the weighted QNN [8], the weighted Schatten p-norm [9], etc, have been proposed to optimize QNN. Another low rank approximation method is low-rank factorization. In [10], the target quaternion matrix is factorized to the product of two small size quaternion matrices such that the low rankness is depicted by this two smaller quaternion matrices. Besides, some classic factorization also have been developed in the quaternion domain. Such as quaternion QR (QQR) decomposition [11], quaternion LU decomposition [12], etc. Further, to optimize the expensive process of obtaining QSVD and improve the efficiency of computation, randomized algorithms is introduced to QSVD [13]. Hereafter, the randomized quaternion QR with Pivoting and Least Squares (QLP) decomposition is proposed to enrich the numerical algorithms of quaternion matrices [14].

In the case of a quaternion tensor, analogous to real tensors, the definition of rank is not unique. Therefore, various factorizations of the quaternion tensor would result in different definitions of rank. The concept of Tucker rank for a quaternion tensor is introduced in [5] for the purpose of handling color images and color videos. In this sense, a color video is seen as a pure quaternion tensor of third order. In addition, a flexible transform-based tensor product called the \star_{QT} -product is introduced, along with its associated Quaternion Tensor Singular Value Decomposition known as TQt-SVD,

as specified in the paper by Miao and Kou [15]. The efficacy of TQt-rank is further demonstrated by the utilization of low-rank approximation in color videos. In addition, the quaternion tensor train is also introduced in the reference [16].

While there has been extensive research on approximating quaternion matrices and quaternion tensors, the majority of studies have mostly concentrated on optimizing low-rank descriptions rather than exploring more efficient factorization approaches. In this paper, the UTV decomposition is specifically developed for quaternion matrices and quaternion tensors to address the existing gap. A UTV decomposition of an $m \times n$ matrix is the result of multiplying an orthogonal matrix \mathbf{U} , a middle triangular matrix \mathbf{T} , and another orthogonal matrix \mathbf{V} together [17, 18, 19]. Hence, the UTV decomposition is classified into two types based on whether the middle triangular matrix is an upper triangular matrix (referred to as URV decomposition) or a lower triangular matrix (referred to as ULV decomposition). Specifically, when considering the URV decomposition of a real matrix \mathbf{A} , the primary computational procedure involves doing the QR with column pivoting (QRCP) decomposition twice: $\mathbf{A}^H = \mathbf{Q}_1 \mathbf{R}_1 \mathbf{P}_1^T$ and $(\mathbf{R}_1 \mathbf{P}_1^T)^H = \mathbf{Q}_2 \mathbf{R}_2 \mathbf{P}_2^T$, where \mathbf{P}_i is permutation matrix. Such that $\mathbf{A} = \mathbf{URV}^H$, where $\mathbf{U} = \mathbf{Q}_2$, $\mathbf{R} = \mathbf{R}_2$, and $\mathbf{V} = \mathbf{Q}_1 \mathbf{P}_2$ [20]. The developed QUTV can be seen as an evolution from UTV in the real domain to UTV in the quaternion domain. Moreover, utilizing the \star_{QT} -product, the QUTV builds up to quaternion tensors. The \star_{QT} -product is defined via a flexible transform. By employing the quaternion Discrete Fourier Transformation (QDFT) and the quaternion Discrete Cosine Transformation (QDCT), among others. The QTUTV algorithm involves reshaping the N th-order quaternion tensor into a third-order quaternion tensor. Then, the QRCP is applied twice to each frontal slice of this modified tensor in the altered domain.

Because the created decomposition acts on the entire original quaternion, the calculation costs are substantial. To achieve more efficient computing, the randomized technique is applied to QUTV and QTUTV. This is prompted by the excellent performance in randomized QSVD [13]. Further, we apply this randomized technique to quaternion tensors. As far as we know, this is the first time the randomized technique has been applied to a quaternion tensor. Moreover, this study analyzes error boundaries and average-case error, building on the work of randomized QSVD in [13] and the real URV decomposition in [21].

To conclude, the primary contribution of this paper can be summarized

as follows.

- The UTV decomposition is proposed for quaternion matrix by employing quaternion QRCP (QQRCP). Further, based on the \star_{QT} -product, the QUTV decomposition is generated to quaternion tensor, named QTUTV.
- In order to enhance the efficiency of algorithms and reduce computational expenses, the QUTV and QTUTV decomposition methods have been supplemented with a randomized approach. In addition, the upper bounds for the proposed methods are given, and the average error bounds on randomized QUTV and randomized QTUTV are established.
- The numerical results demonstrate that the created QUTV achieves comparable relative errors to QSVD while using less time. Similarly, QTUTV can be likened to QTSVD. The efficiency of randomized QUTV and randomized QTUTV is proved in the randomized cases, with an acceptable relative error compared to the randomized QSVD and randomized QTSVD methods, respectively.

The rest of this paper consists of six more sections. Section 2 provides an overview of the relevant notations and fundamental concepts relating to quaternion matrices and quaternion tensors. In Section 3, new quaternion-based QUTV and QTUTV methods are introduced and described in detail. In Section 4, randomized QURV and randomized QTURV are introduced, and theoretical analysis is provided in Section 5. Section 6 demonstrates the effectiveness of the developed methods by comparing numerical experiments with other relevant algorithms. The conclusion is stated in Section 7. Relevant proofs are available in the Appendix.

2. Notations and preliminaries

2.1. Notations

The symbols a , \mathbf{a} , \mathbf{A} , and \mathcal{A} represent scalar, vector, matrix, and tensor quantities in the real number field \mathbb{R} , respectively. The dot notation is employed to represent the scalar, vector, matrix, and tensor variables in the quaternion domain \mathbb{H} . Specifically, \dot{a} denotes a scalar, $\dot{\mathbf{a}}$ represents a vector, $\dot{\mathbf{A}}$ signifies a matrix, and $\dot{\mathcal{A}}$ indicates a tensor. In addition, the complex space

is represented by the symbol \mathbb{C} . The symbol \mathbf{I}_r denotes the identity matrix of size $r \times r$, while $\mathbf{O}_{r_1 \times r_2}$ represents the matrix of zeros with dimensions $r_1 \times r_2$. The symbols $(\cdot)^T$, $(\cdot)^H$, and $(\cdot)^{-1}$ denote the transpose, conjugate transpose, and inverse respectively. The k th frontal slice of an N th-order quaternion tensor $\dot{\mathcal{A}} \in \mathbb{H}^{I_1 \times I_2 \times \dots \times I_N}$ is denoted by $\dot{\mathcal{A}}(:, :, i_3, \dots, i_N)$, and the mode- k unfolding is denoted by $\dot{\mathcal{A}}_{(k)}$. The product of the k -mode is represented by the symbol \times_k . The symbols $\|\cdot\|_F$ and $\|\cdot\|_*$ represent the Frobenius norm and nuclear norm of a given quantity, respectively. The inner product of \cdot_1 and \cdot_2 is defined as $\langle \cdot_1, \cdot_2 \rangle \triangleq \text{tr}(\cdot_1^H \cdot_2)$, and $\text{tr}(\cdot)$ is the trace function.

2.2. Preliminary of quaternion and quaternion matrix

A quaternion number $\dot{a} \in \mathbb{H}$ can be depicted by $\dot{a} = a_0 + a_1 i + a_2 j + a_3 k$, where $a_n \in \mathbb{R}$ ($n = 0, 1, 2, 3$), and i, j, k are three imaginary units which satisfy:

$$\begin{cases} i^2 = j^2 = k^2 = ijk = -1 \\ ij = -ji = k, jk = -kj = i, ki = -ik = j. \end{cases}$$

$\Re(\dot{a}) \triangleq a_0$ and $\Im(\dot{a}) \triangleq a_1 i + a_2 j + a_3 k$ denote the real part and imaginary part of \dot{a} , respectively, so $\dot{a} = \Re(\dot{a}) + \Im(\dot{a})$. When $a_0 = 0$, \dot{a} is a pure quaternion. The conjugate and the modulus of \dot{a} are defined as: $\dot{a}^* = a_0 - a_1 i - a_2 j - a_3 k$ and $|\dot{a}| = \sqrt{\dot{a}\dot{a}^*} = \sqrt{a_0^2 + a_1^2 + a_2^2 + a_3^2}$, separately. It is essential to acknowledge that multiplication in the quaternion domain does not adhere to the commutative property, *i.e.* $\dot{a}\dot{b} \neq \dot{b}\dot{a}$.

A quaternion matrix $\dot{\mathbf{A}} = (\dot{a}_{ij}) \in \mathbb{H}^{M \times N}$, where $\dot{\mathbf{A}} = \mathbf{A}_0 + \mathbf{A}_1 i + \mathbf{A}_2 j + \mathbf{A}_3 k$, and $\mathbf{A}_n \in \mathbb{R}^{M \times N}$ ($n = 0, 1, 2, 3$). The conjugate transpose of $\dot{\mathbf{A}}$ is $\dot{\mathbf{A}}^H = \mathbf{A}_0^T - \mathbf{A}_1^T i - \mathbf{A}_2^T j - \mathbf{A}_3^T k$. The Frobenius norm is defined as: $\|\dot{\mathbf{A}}\|_F = \sqrt{\sum_{i=1}^M \sum_{j=1}^N |\dot{a}_{ij}|^2} = \sqrt{\text{tr}(\dot{\mathbf{A}}^H \dot{\mathbf{A}})}$. The spectral norm is defined as: $\|\dot{\mathbf{A}}\|_2 = \max_{\mathbf{x} \in \mathbb{H}^N, \|\mathbf{x}\|_2=1} \|\dot{\mathbf{A}}\mathbf{x}\|_2$, where the 2-norm is: $\|\dot{\mathbf{A}}\mathbf{x}\|_2 = (\sum_{i=1}^N |\dot{\mathbf{A}}\mathbf{x}_i|^2)^{\frac{1}{2}}$.

Definition 1. (*The rank of quaternion matrix [22]*): For a quaternion matrix $\dot{\mathbf{A}} = (\dot{a}_{ij}) \in \mathbb{H}^{M \times N}$, the maximum number of right (left) linearly independent columns (rows) is defined as the rank of $\dot{\mathbf{A}}$.

Theorem 1. (*QSVD [22]*): Let a quaternion matrix $\dot{\mathbf{A}} \in \mathbb{H}^{M \times N}$ be of rank r . There exist two unitary quaternion matrices $\dot{\mathbf{U}} \in \mathbb{H}^{M \times M}$ and $\dot{\mathbf{V}} \in \mathbb{H}^{N \times N}$ such that

$$\dot{\mathbf{A}} = \dot{\mathbf{U}} \begin{pmatrix} \Sigma_r & \mathbf{0} \\ \mathbf{0} & \mathbf{0} \end{pmatrix} \dot{\mathbf{V}}^H = \dot{\mathbf{U}} \Lambda \dot{\mathbf{V}}^H, \quad (1)$$

where $\Sigma_r = \text{diag}(\sigma_1, \dots, \sigma_r) \in \mathbb{R}^{r \times r}$, and all singular values $\sigma_i > 0, i = 1, \dots, r$.

2.3. Preliminary of quaternion tensor

Definition 2 (Quaternion tensor[5]). A multi-dimensional array or an N th-order tensor is referred to as a quaternion tensor when its elements are quaternions. Specifically, quaternion tensor $\dot{\mathcal{A}} = (\dot{a}_{i_1 i_2 \dots i_N}) \in \mathbb{H}^{I_1 \times I_2 \times \dots \times I_N}$ is formulated as $\dot{\mathcal{A}} = \mathcal{A}_0 + \mathcal{A}_1 i + \mathcal{A}_2 j + \mathcal{A}_3 k$, where $\mathcal{A}_n \in \mathbb{R}^{I_1 \times I_2 \times \dots \times I_N}$ ($n = 0, 1, 2, 3$) are real tensors.

Definition 3 (\star_{QT} -product [15]). Given two N th-order ($N \geq 3$) quaternion tensors $\dot{\mathcal{A}} \in \mathbb{H}^{I_1 \times I_2 \times \dots \times I_N}$, $\dot{\mathcal{B}} \in \mathbb{H}^{I_1 \times I_2 \times \dots \times I_N}$ and $N - 2$ invertible quaternion matrices $\dot{\mathcal{Q}}_3 \in \mathbb{H}^{I_3 \times I_3}, \dots, \dot{\mathcal{Q}}_N \in \mathbb{H}^{I_N \times I_N}$, the \star_{QT} -product is defined as

$$\dot{\mathcal{T}} = \dot{\mathcal{A}} \star_{QT} \dot{\mathcal{B}} = (\hat{\mathcal{A}} \star_{QF} \hat{\mathcal{B}}) \times_3 \dot{\mathcal{Q}}_3^{-1} \times_4 \dots \times_N \dot{\mathcal{Q}}_N^{-1}, \quad (2)$$

where $\hat{\mathcal{A}} = \dot{\mathcal{A}} \times_3 \dot{\mathcal{Q}}_3 \times_4 \dots \times_N \dot{\mathcal{Q}}_N$ and $\hat{\mathcal{B}} = \dot{\mathcal{B}} \times_3 \dot{\mathcal{Q}}_3 \times_4 \dots \times_N \dot{\mathcal{Q}}_N$. The \star_{QF} -product is the quaternion facewise produce, i.e., $\dot{\mathcal{F}} = \dot{\mathcal{A}} \star_{QF} \dot{\mathcal{B}}$ such that the frontal slice of $\dot{\mathcal{F}}$ satisfies $\dot{\mathcal{F}}(:, :, i_3, \dots, i_N) = \dot{\mathcal{A}}(:, :, i_3, \dots, i_N) \dot{\mathcal{B}}(:, :, i_3, \dots, i_N)$.

Remark 1. Based on \star_{QT} -product, the conjugate transpose of $\dot{\mathcal{A}}$ is denoted by $\dot{\mathcal{A}}^H$ and satisfies $\dot{\mathcal{A}}^H(:, :, i_3, \dots, i_N) = (\dot{\mathcal{A}}(:, :, i_3, \dots, i_N))^H$. The identity quaternion tensor $\dot{\mathcal{I}} \in \mathbb{H}^{I_1 \times I_2 \times \dots \times I_N}$ has the property that $\dot{\mathcal{I}}(:, :, i_3, \dots, i_N) = \dot{\mathbf{I}} \in \mathbb{H}^{I_1 \times I_2}$. If a quaternion tensor $\dot{\mathcal{U}} \in \mathbb{H}^{I_1 \times I_2 \times \dots \times I_N}$ satisfies $\dot{\mathcal{U}} \star_{QT} \dot{\mathcal{U}}^H = \dot{\mathcal{I}} = \dot{\mathcal{U}}^H \star_{QT} \dot{\mathcal{U}}$, $\dot{\mathcal{U}}$ is a unitary quaternion tensor.

Theorem 2 (TQt-SVD [15]). Let $\dot{\mathcal{T}} \in \mathbb{H}^{I_1 \times I_2 \times \dots \times I_N}$ ($N \geq 3$). There exist two unitary quaternion tensors $\dot{\mathcal{U}} \in \mathbb{H}^{I_1 \times I_1 \times \dots \times I_N}$, and $\dot{\mathcal{V}} \in \mathbb{H}^{I_2 \times I_2 \times \dots \times I_N}$. Such that

$$\dot{\mathcal{T}} = \dot{\mathcal{U}} \star_{QT} \dot{\mathcal{D}} \star_{QT} \dot{\mathcal{V}}^H,$$

where the tensor $\dot{\mathcal{D}} \in \mathbb{H}^{I_1 \times I_2 \times \dots \times I_N}$ is an f -diagonal quaternion tensor, which means that only the diagonal components of its frontal slices have non-zero values.

Definition 4 (TQt-rank [15]). Let $\dot{\mathcal{T}} \in \mathbb{H}^{I_1 \times I_2 \times \dots \times I_N}$ ($N \geq 3$), and the corresponding TQt-SVD is $\dot{\mathcal{T}} = \dot{\mathcal{U}} \star_{QT} \dot{\mathcal{D}} \star_{QT} \dot{\mathcal{V}}^H$. The TQt-rank of $\dot{\mathcal{T}}$ is defined as the number of nonzero tubes in $\dot{\mathcal{D}}$, i.e., $\text{rank}_{TQt}(\dot{\mathcal{T}}) = \#\{k \mid \|\dot{\mathcal{D}}(k, k, :, \dots, :)\|_F > 0\}, k \in [K], K = \min\{I_1, I_2\}$. Moreover, the k th singular value of $\dot{\mathcal{T}}$ is defined as $\sigma_k(\dot{\mathcal{T}}) = \|\dot{\mathcal{D}}(k, k, :, \dots, :)\|_F$.

Additional details on quaternions, quaternion matrices, and quaternion tensors can be found in the following references: [5, 15, 22].

3. Quaternion UTV decompositions

3.1. Quaternion matrix UTV decomposition

Analogy to the real cases, the QUTV decomposition of a quaternion matrix can be divided into two classes. For a quaternion matrix $\dot{\mathbf{A}} \in \mathbb{H}^{M \times N}$, the QUTV decomposition is $\dot{\mathbf{A}} = \dot{\mathbf{U}}\dot{\mathbf{T}}\dot{\mathbf{V}}^H$, where $\dot{\mathbf{U}} \in \mathbb{H}^{M \times M}$, $\dot{\mathbf{V}} \in \mathbb{H}^{N \times N}$ are two unitary quaternion matrices, and $\dot{\mathbf{T}} \in \mathbb{H}^{M \times N}$ is a triangular quaternion matrix. The QURV decomposition is formulated as follows when $\dot{\mathbf{T}}$ is upper triangular.

$$\dot{\mathbf{A}} = \dot{\mathbf{U}} \begin{pmatrix} \dot{\mathbf{T}}_{11} & \dot{\mathbf{T}}_{12} \\ \mathbf{0}_{(M-K) \times (K)} & \dot{\mathbf{T}}_{22} \end{pmatrix} \dot{\mathbf{V}}^H, \quad (3)$$

where $\dot{\mathbf{T}}_{11} \in \mathbb{H}^{K \times K}$, $\dot{\mathbf{T}}_{12} \in \mathbb{H}^{K \times (N-K)}$, and $\dot{\mathbf{T}}_{22} \in \mathbb{H}^{(M-K) \times (N-K)}$. The QULV decomposition is formulated as follows when $\dot{\mathbf{T}}$ is lower triangular.

$$\dot{\mathbf{A}} = \dot{\mathbf{U}} \begin{pmatrix} \dot{\mathbf{T}}_{11} & \mathbf{0}_{K \times (N-K)} \\ \dot{\mathbf{T}}_{21} & \dot{\mathbf{T}}_{22} \end{pmatrix} \dot{\mathbf{V}}^H \quad (4)$$

where $\dot{\mathbf{T}}_{11} \in \mathbb{H}^{K \times K}$, $\dot{\mathbf{T}}_{21} \in \mathbb{H}^{(M-K) \times K}$, and $\dot{\mathbf{T}}_{22} \in \mathbb{H}^{(M-K) \times (N-K)}$.

Basing on the above situation, when the middle quaternion matrix is diagonal and the elements are real nonnegative, the decomposition is referred as QSVD.

$$\dot{\mathbf{A}} = \dot{\mathbf{U}} \begin{pmatrix} \dot{\mathbf{T}}_{11} & \mathbf{0}_{K \times (N-K)} \\ \mathbf{0}_{(M-K) \times K} & \dot{\mathbf{T}}_{22} \end{pmatrix} \dot{\mathbf{V}}^H. \quad (5)$$

In this case, the diagonal elements in $\dot{\mathbf{T}}$ are singular values of $\dot{\mathbf{A}}$, and $\dot{\mathbf{A}}_K = \dot{\mathbf{U}}(:, 1 : K)\dot{\mathbf{T}}_{11}\dot{\mathbf{V}}(:, 1 : K)^H$ provides the best rank-K approximation for $\dot{\mathbf{A}}$ [23].

As stated in Section 2, an efficient method for computing URV decomposition can be performed by employing QRCP. Furthermore, by utilizing the QQRCP, Algorithm 1 presents a concise description of the procedure for QURV decomposition. Similarly, the QULV decomposition is described in detail in Algorithm 2.

Algorithm 1 The QURV decomposition

Input: Quaternion matrix data $\dot{\mathbf{A}} \in \mathbb{H}^{M \times N}$.

Output: Two unitary quaternion matrices: $\dot{\mathbf{U}} \in \mathbb{H}^{M \times M}$, $\dot{\mathbf{V}} \in \mathbb{H}^{N \times N}$ and an upper triangular quaternion matrix $\dot{\mathbf{R}} \in \mathbb{H}^{M \times N}$ such that $\dot{\mathbf{A}} = \dot{\mathbf{U}}\dot{\mathbf{R}}\dot{\mathbf{V}}^H$.

- 1: Compute the QRCP of $\dot{\mathbf{A}}^H$ as $\dot{\mathbf{A}}^H = \dot{\mathbf{Q}}_1\dot{\mathbf{R}}_1\mathbf{P}_1^T$.
 - 2: Compute the QRCP of $(\dot{\mathbf{R}}_1\mathbf{P}_1^T)^H$ as $(\dot{\mathbf{R}}_1\mathbf{P}_1^T)^H = \dot{\mathbf{Q}}_2\dot{\mathbf{R}}_2\mathbf{P}_2^T$.
 - 3: $\dot{\mathbf{U}} = \dot{\mathbf{Q}}_2$, $\dot{\mathbf{R}} = \dot{\mathbf{R}}_2$, and $\dot{\mathbf{V}} = \dot{\mathbf{Q}}_1\mathbf{P}_2$.
-

Algorithm 2 The QULV decomposition

Input: Quaternion matrix data $\dot{\mathbf{A}} \in \mathbb{H}^{M \times N}$.

Output: Two unitary quaternion matrices: $\dot{\mathbf{U}} \in \mathbb{H}^{M \times M}$, $\dot{\mathbf{V}} \in \mathbb{H}^{N \times N}$ and a lower triangular quaternion matrix $\dot{\mathbf{L}} \in \mathbb{H}^{M \times N}$ such that $\dot{\mathbf{A}} = \dot{\mathbf{U}}\dot{\mathbf{L}}\dot{\mathbf{V}}^H$.

- 1: Compute the QRCP of $\dot{\mathbf{A}}$ as $\dot{\mathbf{A}} = \dot{\mathbf{Q}}_1\dot{\mathbf{R}}_1\mathbf{P}_1^T$.
 - 2: Compute the QRCP of $(\dot{\mathbf{R}}_1\mathbf{P}_1^T)^H$ as $(\dot{\mathbf{R}}_1\mathbf{P}_1^T)^H = \dot{\mathbf{Q}}_2\dot{\mathbf{R}}_2\mathbf{P}_2^T$.
 - 3: $\dot{\mathbf{U}} = \dot{\mathbf{Q}}_1\mathbf{P}_2$, $\dot{\mathbf{L}} = \dot{\mathbf{R}}_2^H$, and $\dot{\mathbf{V}} = \dot{\mathbf{Q}}_2$.
-

3.2. Quaternion tensor *UTV* decomposition

Based on the \star_{QT} -product, the following QTUTV decomposition is proposed for N th-order quaternion tensor.

Theorem 3 (QTUTV). *Let $\dot{\mathcal{T}} \in \mathbb{H}^{I_1 \times I_2 \times \dots \times I_N}$ ($N \geq 3$). $\dot{\mathcal{T}}$ can be decomposed to*

$$\dot{\mathcal{A}} = \dot{\mathcal{U}} \star_{QT} \dot{\mathcal{T}} \star_{QT} \dot{\mathcal{V}}^H,$$

where $\dot{\mathcal{U}} \in \mathbb{H}^{I_1 \times I_1 \times \dots \times I_N}$, and $\dot{\mathcal{V}} \in \mathbb{H}^{I_2 \times I_2 \times \dots \times I_N}$ are unitary quaternion tensors, and $\dot{\mathcal{T}} \in \mathbb{H}^{I_1 \times I_2 \times \dots \times I_N}$ is a frontal triangular quaternion tensor, indicating that the frontal slices of $\dot{\mathcal{T}}$ are triangular.

Remark 2. *When the frontal triangular quaternion tensor $\dot{\mathcal{T}}$ is f -upper triangular (meaning that the frontal slices are of upper triangular quaternion matrices), the QTUTV decomposition is equivalent to QTURV decomposition. Similarly, when the triangular quaternion tensor $\dot{\mathcal{T}}$ is f -lower triangular (meaning that frontal slices are of lower triangular quaternion matrices), the QTUTV decomposition is equivalent to QTULV decomposition. Moreover, if the triangular quaternion tensor $\dot{\mathcal{T}}$ satisfies the condition of being f -diagonal triangular (i.e., the frontal slices consist of diagonal quaternion matrices), then the QTUTV decomposition can be referred to as the QTSVD decomposition.*

Algorithm 3 summarizes the QTURV decomposition using QQRCP decomposition for each frontal slice of the quaternion tensor in the transform domain. The algorithmic procedure of QTULV is analogous and will not be reiterated here.

Algorithm 3 The QTURV decomposition

Input: Quaternion tensor data $\hat{\mathcal{A}} \in \mathbb{H}^{I_1 \times I_2 \times \dots \times I_N}$ ($N \geq 3$), and invertible quaternion matrices $\dot{\mathbf{Q}}_3 \in \mathbb{H}^{I_3 \times I_3}, \dots, \dot{\mathbf{Q}}_N \in \mathbb{H}^{I_N \times I_N}$.

Output: Two unitary quaternion tensors: $\dot{\mathcal{U}} \in \mathbb{H}^{I_1 \times I_1 \times \dots \times I_N}$, $\dot{\mathcal{V}} \in \mathbb{H}^{I_2 \times I_2 \times \dots \times I_N}$, and a f-upper quaternion tensor $\dot{\mathcal{R}} \in \mathbb{H}^{I_1 \times I_2 \times \dots \times I_N}$ such that $\hat{\mathcal{A}} = \dot{\mathcal{U}} \star_{QT} \dot{\mathcal{T}} \star_{QT} \dot{\mathcal{V}}^H$.

- 1: Convert $\hat{\mathcal{A}}$ to transform domain: $\hat{\hat{\mathcal{A}}} = \hat{\mathcal{A}} \times_3 \dot{\mathbf{Q}}_3 \times_4 \dots \times_N \dot{\mathbf{Q}}_N$.
 - 2: Concatenate frontal slices along the third dimension:
 $\hat{\hat{\mathcal{A}}} = \text{reshape}(\hat{\mathcal{A}}, [I_1, I_2, I_3 I_4 \dots I_N])$.
 - 3: **for** $k=1:I_3 I_4 \dots I_N$ **do**
 - 4: Compute the QQRCP of $\hat{\hat{\mathcal{A}}}(:, :, k)^H$:
 $\hat{\hat{\mathcal{A}}}(:, :, k)^H = \hat{\hat{\mathcal{Q}}}_1(:, :, k) \hat{\hat{\mathcal{R}}}_1(:, :, k) \mathcal{P}_1(:, :, k)^T$.
 - 5: Compute the QQRCP of $(\hat{\hat{\mathcal{R}}}_1(:, :, k) \mathcal{P}_1(:, :, k)^T)^H$:
 $(\hat{\hat{\mathcal{R}}}_1(:, :, k) \mathcal{P}_1(:, :, k)^T)^H = \hat{\hat{\mathcal{Q}}}_2(:, :, k) \hat{\hat{\mathcal{R}}}_2(:, :, k) \mathcal{P}_2(:, :, k)^T$.
 - 6: **end for**
 - 7: Reshape into N th-order quaternion tensors:
 $\hat{\hat{\mathcal{U}}} = \text{reshape}(\hat{\hat{\mathcal{Q}}}_2, [I_1, I_1, I_3, \dots, I_N])$;
 $\hat{\hat{\mathcal{R}}} = \text{reshape}(\hat{\hat{\mathcal{R}}}_2, [I_1, I_2, I_3, \dots, I_N])$;
 $\hat{\hat{\mathcal{V}}} = \text{reshape}(\hat{\hat{\mathcal{Q}}}_1 \star_{QF} \mathcal{P}_2, [I_2, I_2, I_3, \dots, I_N])$.
 - 8: Return to the original domain:
 $\dot{\mathcal{U}} = \hat{\hat{\mathcal{U}}} \times_3 \dot{\mathbf{Q}}_3^{-1} \times_4 \dots \times_N \dot{\mathbf{Q}}_N^{-1}$;
 $\dot{\mathcal{R}} = \hat{\hat{\mathcal{R}}} \times_3 \dot{\mathbf{Q}}_3^{-1} \times_4 \dots \times_N \dot{\mathbf{Q}}_N^{-1}$;
 $\dot{\mathcal{V}} = \hat{\hat{\mathcal{V}}} \times_3 \dot{\mathbf{Q}}_3^{-1} \times_4 \dots \times_N \dot{\mathbf{Q}}_N^{-1}$.
-

4. Randomized quaternion UTV decompositions

This section is dedicated to the development of randomized QURV and QTURV for the purpose of computing the decomposition in a more efficient

manner. This technique is determined by the chosen rank and utilizes a randomized test quaternion matrix with QQR decomposition. The method used for a quaternion matrix is called Compressed Randomized QURV (CoR-QURV), and the approach used for a quaternion tensor is called Compressed Randomized QTURV (CoR-QTURV).

4.1. Randomized Algorithms for QURV

Given a quaternion matrix $\dot{\mathbf{A}} \in \mathbb{H}^{M \times N}$, two integers l and p , where l is the target rank and p is the power scheme parameter. Forming an $N \times l$ quaternion random test matrix as $\dot{\mathbf{\Omega}} = \dot{\mathbf{\Omega}}_0 + \dot{\mathbf{\Omega}}_1 i + \dot{\mathbf{\Omega}}_2 j + \dot{\mathbf{\Omega}}_3 k$, where $\dot{\mathbf{\Omega}}_i, i = 0, 1, 2, 3$ are random and independently drawn from the $N(0, 1)$ -normal distribution. Then, the whole process of CoR-QURV can be summarized in Algorithm 4.

Algorithm 4 The CoR-QURV decomposition

Input: Quaternion matrix data $\dot{\mathbf{A}} \in \mathbb{H}^{M \times N}$, integers l and the power parameter p .

Output: Two unitary quaternion matrices: $\dot{\mathbf{U}} \in \mathbb{H}^{M \times l}$, $\dot{\mathbf{V}} \in \mathbb{H}^{l \times N}$ and an upper triangular quaternion matrix $\dot{\mathbf{R}} \in \mathbb{H}^{l \times l}$ such that $\dot{\mathbf{A}} \approx \dot{\mathbf{U}} \dot{\mathbf{R}} \dot{\mathbf{V}}^H$.

- 1: Draw an $N \times l$ quaternion random test matrix $\dot{\mathbf{\Omega}}$.
 - 2: Construct $\dot{\mathbf{Y}}_0 = \dot{\mathbf{A}} \dot{\mathbf{\Omega}}$.
 - 3: **for** $i = 1 : p$ **do**
 - 4: Compute $\hat{\mathbf{Y}}_i = \dot{\mathbf{A}}^H \dot{\mathbf{Y}}_{i-1}$ and $\dot{\mathbf{Y}}_i = \dot{\mathbf{A}} \hat{\mathbf{Y}}_i$.
 - 5: **end for**
 - 6: Compute the QQR of $\hat{\mathbf{Y}}_q$ and $\dot{\mathbf{Y}}_q$ as $\hat{\mathbf{Y}}_q = \dot{\mathbf{Q}}_1 \dot{\mathbf{R}}_1$ and $\dot{\mathbf{Y}}_q = \dot{\mathbf{Q}}_2 \dot{\mathbf{R}}_2$.
 - 7: Compute the QQRCQP of $\dot{\mathbf{M}} = \dot{\mathbf{Q}}_1^H \dot{\mathbf{A}} \dot{\mathbf{Q}}_2$ as $\dot{\mathbf{M}} = \dot{\mathbf{Q}}_3 \dot{\mathbf{R}}_3 \dot{\mathbf{P}}^T$.
 - 8: Form the CoR-QURV decomposition of $\dot{\mathbf{A}}$, $\dot{\mathbf{U}} = \dot{\mathbf{Q}}_1 \dot{\mathbf{Q}}_3$, $\dot{\mathbf{R}} = \dot{\mathbf{R}}_3$, and $\dot{\mathbf{V}} = \dot{\mathbf{Q}}_2 \dot{\mathbf{P}}$.
-

Remark 3. For the 7th step in Algorithm 4, when $p = 1$, multiplying $\dot{\mathbf{Q}}_2^H \dot{\mathbf{\Omega}}$, then the equation can be rewritten as $\dot{\mathbf{M}} \dot{\mathbf{Q}}_2 \dot{\mathbf{\Omega}} = \dot{\mathbf{Q}}_1^H \dot{\mathbf{A}} \dot{\mathbf{Q}}_2 \dot{\mathbf{Q}}_2^H \dot{\mathbf{\Omega}}$. Assuming $\dot{\mathbf{A}} \approx \dot{\mathbf{A}} \dot{\mathbf{Q}}_2 \dot{\mathbf{Q}}_2^H$, the quaternion matrix $\dot{\mathbf{Q}}_1^H \dot{\mathbf{A}} \dot{\mathbf{Q}}_2$ can be replaced by $\dot{\mathbf{Q}}_1^H \dot{\mathbf{Y}}_0 (\dot{\mathbf{Q}}_2^H \dot{\mathbf{\Omega}})^\dagger$ which requires $\mathcal{O}(Ml^2 + l^3 + Nl^2)$. However, the computational complexity of computing $(\dot{\mathbf{Q}}_1^H \dot{\mathbf{A}}) \dot{\mathbf{Q}}_2$ and $\dot{\mathbf{Q}}_1^H (\dot{\mathbf{A}} \dot{\mathbf{Q}}_2)$ is $\mathcal{O}(Mnl + Nl^2)$ and $\mathcal{O}(Mnl + Ml^2)$, respectively. When $l < \min(M, N)$, the cost of obtaining $\dot{\mathbf{Q}}_1^H \dot{\mathbf{Y}}_0 (\dot{\mathbf{\Omega}})^\dagger \dot{\mathbf{Q}}_2$ is less than the cost of obtaining $\dot{\mathbf{Q}}_1^H \dot{\mathbf{A}} \dot{\mathbf{Q}}_2$.

The computational complexity of each step in Algorithm 4 is assessed. In the first step, drawing a quaternion random test matrix Ω needs $\mathcal{O}(Ml)$. Then, the computational complexity for forming $\hat{\mathbf{Y}}_i$ and $\check{\mathbf{Y}}_i$ both are $\mathcal{O}(Ml^2)$. The costs of QQR decomposition are $\mathcal{O}(Ml^2)$ and $\mathcal{O}(Nl^2)$, then computing the multiplication of $(\dot{\mathbf{Q}}_1^H \dot{\mathbf{A}}) \dot{\mathbf{Q}}_2$ and QQRCP need $\mathcal{O}(MNI + Nl^2)$ and $\mathcal{O}(l^3)$, respectively. At last, forming $\dot{\mathbf{U}}$ and $\dot{\mathbf{V}}$ require $\mathcal{O}(Ml^2)$ and $\mathcal{O}(Nl)$, respectively. Hence, the cost of CoR-QURV is $\mathcal{O}(Ml + Nl + MNI + 3Ml^2 + 2Nl^2 + l^3)$.

4.2. Randomized Algorithms for QTURV

Similar to the proposed QTURV decomposition, the following CoR-QTURV decomposition is developed for N th-order quaternion tensor.

The computational complexity of each step in Algorithm 5 is assessed. Let a quaternion tensor $\hat{\mathbf{A}} \in \mathbb{H}^{I_1 \times I_2 \times I_3}$ as an example, and the transformation used in the following experiment is Quaternion Discrete Cosine Transform (QDCT). In the first step, drawing a quaternion random test matrix Ω needs $\mathcal{O}(I_2l)$, and converting $\hat{\mathbf{A}}$ to transform domain needs $\mathcal{O}(I_1I_2I_3 \log(I_3))$. Then, the computational complexity for forming $\hat{\mathbf{Y}}_i^k$ and $\check{\mathbf{Y}}_i^k$ both is $\mathcal{O}(I_1I_2I_3l)$. The costs of QQR decomposition is $\mathcal{O}(I_1I_3l^2)$ and $\mathcal{O}(I_2I_3l^2)$, then computing the multiplication of $(\dot{\mathbf{Q}}_1^H \dot{\mathbf{A}}) \dot{\mathbf{Q}}_2$ and QQRCP need $\mathcal{O}(I_1I_2I_3l + I_2I_3l^2)$ and $\mathcal{O}(I_3l^3)$, respectively. Then, forming $\tilde{\mathbf{U}}$ and $\tilde{\mathbf{V}}$ require $\mathcal{O}(I_1I_3l^2)$ and $\mathcal{O}(I_2I_3l)$, respectively. At last, the computational complexity for transforming $\tilde{\mathbf{U}}, \tilde{\mathbf{R}}$ and $\tilde{\mathbf{V}}$ to the original domain is $\mathcal{O}(I_1I_3l \log(I_3))$, $\mathcal{O}(I_2I_3l \log(I_3))$, and $\mathcal{O}(I_3l^2 \log(I_3))$, respectively. Hence, the computational complexity of CoR-QURV is $\mathcal{O}(I_2l + I_1I_2I_3 \log(I_3) + 2I_1I_3l^2 + 2I_2I_3l^2 + I_1I_2I_3l + I_2I_3l + I_3l^3 + I_1I_3l \log(I_3) + I_2I_3l \log(I_3) + I_3l^2 \log(I_3))$.

Remark 4. Let a quaternion tensor $\hat{\mathbf{A}} \in \mathbb{H}^{I_1 \times I_2 \times I_3}$ as an example. For the 10th step in Algorithm 5, when $p = 1$, the quaternion matrix $\dot{\mathbf{Q}}_1^{kH} \hat{\mathbf{A}}(:, :, k) \mathbf{Q}_2^k$ can be replaced by $\dot{\mathbf{Q}}_1^{kH} \check{\mathbf{Y}}_0^k (\dot{\mathbf{Q}}_2^{kH} \dot{\Omega})^\dagger$ which requires $\mathcal{O}(I_1l^2 + l^3 + I_2l^2)$ computational complexity for every k . However, the computational complexity of computing $(\dot{\mathbf{Q}}_1^{kH} \hat{\mathbf{A}}(:, :, k)) \mathbf{Q}_2^k$ and $\dot{\mathbf{Q}}_1^{kH} (\hat{\mathbf{A}}(:, :, k) \mathbf{Q}_2^k)$ is $\mathcal{O}(I_1I_2l + I_2l^2)$ and $\mathcal{O}(I_1I_2l + I_1l^2)$, respectively. When $l < \min(I_1, I_2)$, the cost of obtaining $\dot{\mathbf{Q}}_1^{kH} \check{\mathbf{Y}}_0^k (\dot{\Omega})^\dagger \dot{\mathbf{Q}}_2^k$ is less than the cost of obtaining $\dot{\mathbf{Q}}_1^{kH} \hat{\mathbf{A}}(:, :, k) \mathbf{Q}_2^k$.

5. Theoretical Analysis

In this section, the theoretical analysis of the above algorithms are giving, including the low-rank approximation of the randomized methods. These ap-

Algorithm 5 The CoR-QTURV decomposition

Input: Quaternion tensor data $\hat{\mathcal{A}} \in \mathbb{H}^{I_1 \times I_2 \times \dots \times I_N}$ ($N \geq 3$), and invertible quaternion matrices $\hat{\mathbf{Q}}_3 \in \mathbb{H}^{I_3 \times I_3}, \dots, \hat{\mathbf{Q}}_N \in \mathbb{H}^{I_N \times I_N}$. Integers l and the power parameter p .

Output: Two unitary quaternion tensors: $\hat{\mathcal{U}} \in \mathbb{H}^{I_1 \times l \times \dots \times I_N}$, $\hat{\mathcal{V}} \in \mathbb{H}^{I_2 \times l \times \dots \times I_N}$, and a f-upper quaternion tensor $\hat{\mathcal{R}} \in \mathbb{H}^{l \times l \times \dots \times I_N}$ such that $\hat{\mathcal{A}} \approx \hat{\mathcal{U}} \star_{QT} \hat{\mathcal{T}} \star_{QT} \hat{\mathcal{V}}^H$.

- 1: Draw an $I_2 \times l$ quaternion random test matrix $\hat{\mathbf{\Omega}}$.
 - 2: Convert $\hat{\mathcal{A}}$ to transform domain: $\hat{\hat{\mathcal{A}}} = \hat{\mathcal{A}} \times_3 \hat{\mathbf{Q}}_3 \times_4 \dots \times_N \hat{\mathbf{Q}}_N$.
 - 3: Concatenate frontal slices along the third dimension:
 $\hat{\hat{\mathcal{A}}} = \text{reshape}(\hat{\hat{\mathcal{A}}}, [I_1, I_2, I_3 I_4 \dots I_N])$.
 - 4: **for** $k=1:I_3 I_4 \dots I_N$ **do**
 - 5: Construct $\hat{\mathbf{Y}}_0^k = \hat{\hat{\mathcal{A}}}(:, :, k) \hat{\mathbf{\Omega}}$.
 - 6: **for** $i = 1 : p$ **do**
 - 7: Compute $\hat{\mathbf{Y}}_i^k = \hat{\hat{\mathcal{A}}}(:, :, k)^H \hat{\mathbf{Y}}_{i-1}^k$ and $\hat{\mathbf{Y}}_i^k = \hat{\hat{\mathcal{A}}}(:, :, k) \hat{\mathbf{Y}}_i^k$.
 - 8: **end for**
 - 9: Compute the QQR of $\hat{\mathbf{Y}}_q^k$ and $\hat{\mathbf{Y}}_q^k$ as $\hat{\mathbf{Y}}_q^k = \hat{\mathbf{Q}}_1^k \hat{\mathbf{R}}_1^k$ and $\hat{\mathbf{Y}}_q^k = \hat{\mathbf{Q}}_2^k \hat{\mathbf{R}}_2^k$.
 - 10: Compute the QQRCP of $\hat{\mathbf{M}}^k = \hat{\mathbf{Q}}_1^{kH} \hat{\hat{\mathcal{A}}}(:, :, k) \hat{\mathbf{Q}}_2^k$ as $\hat{\mathbf{M}}^k = \hat{\mathbf{Q}}_3^k \hat{\mathbf{R}}_3^k \hat{\mathbf{P}}^{kT}$.
 - 11: Let $\hat{\mathcal{U}}(:, :, k) = \hat{\mathbf{Q}}_1^k \hat{\mathbf{Q}}_3^k$, $\hat{\mathcal{R}}(:, :, k) = \hat{\mathbf{R}}_3^k$, $\hat{\mathcal{V}}(:, :, k) = \hat{\mathbf{Q}}_2^k \hat{\mathbf{P}}^k$
 - 12: **end for**
 - 13: Reshape into N th-order quaternion tensors:
 $\hat{\hat{\mathcal{U}}} = \text{reshape}(\hat{\mathcal{U}}(:, :, k), [I_1, l, I_3, \dots, I_N])$;
 $\hat{\hat{\mathcal{R}}} = \text{reshape}(\hat{\mathcal{R}}(:, :, k), [l, l, I_3, \dots, I_N])$;
 $\hat{\hat{\mathcal{V}}} = \text{reshape}(\hat{\mathcal{V}}(:, :, k), [I_2, l, I_3, \dots, I_N])$.
 - 14: Return to the original domain:
 $\hat{\mathcal{U}} = \hat{\hat{\mathcal{U}}} \times_3 \hat{\mathbf{Q}}_3^{-1} \times_4 \dots \times_N \hat{\mathbf{Q}}_N^{-1}$;
 $\hat{\mathcal{R}} = \hat{\hat{\mathcal{R}}} \times_3 \hat{\mathbf{Q}}_3^{-1} \times_4 \dots \times_N \hat{\mathbf{Q}}_N^{-1}$;
 $\hat{\mathcal{V}} = \hat{\hat{\mathcal{V}}} \times_3 \hat{\mathbf{Q}}_3^{-1} \times_4 \dots \times_N \hat{\mathbf{Q}}_N^{-1}$.
-

proximations are backed by theoretical assurances that ensure their accuracy in term of the Frobenius norm. To achieve this objective, a theorem initially is provided.

Theorem 4. Let $\dot{\mathbf{Q}}_1 \in \mathbb{H}^{M \times l}$, $\dot{\mathbf{Q}}_2 \in \mathbb{H}^{N \times l}$ be quaternion matrices constructed by Algorithm 4. Let $\dot{\mathbf{M}}_K$ be the best rank- K approximation of $\dot{\mathbf{Q}}_1^H \dot{\mathbf{A}} \dot{\mathbf{Q}}_2 \in \mathbb{H}^{l \times l}$. Then, $\dot{\mathbf{M}}_K$ is an optimal solution of the following optimization problem:

$$\min_{\mathbf{M}, \text{rank}(\mathbf{M}) \leq k} \|\dot{\mathbf{A}} - \dot{\mathbf{Q}}_1 \dot{\mathbf{M}} \dot{\mathbf{Q}}_2^H\|_F = \|\dot{\mathbf{A}} - \dot{\mathbf{Q}}_1 \dot{\mathbf{M}}_K \dot{\mathbf{Q}}_2^H\|_F, \quad (6)$$

besides,

$$\|\dot{\mathbf{A}} - \dot{\mathbf{Q}}_1 \dot{\mathbf{M}}_K \dot{\mathbf{Q}}_2^H\|_F \leq \|\dot{\mathbf{A}} - \dot{\mathbf{A}}_K\|_F + \|\dot{\mathbf{A}}_K - \dot{\mathbf{Q}}_1 \dot{\mathbf{Q}}_1^H \dot{\mathbf{A}}_K\|_F + \|\dot{\mathbf{A}}_K - \dot{\mathbf{A}}_K \dot{\mathbf{Q}}_2 \dot{\mathbf{Q}}_2^H\|_F. \quad (7)$$

Proof: Because the signal total energy computed in the spatial domain and the quaternion domain are equal, according to the Parseval theorem in the quaternion domain [24, 25]. The following relations are hold.

$$\begin{aligned} \|\dot{\mathbf{A}} - \dot{\mathbf{Q}}_1 \dot{\mathbf{M}} \dot{\mathbf{Q}}_2^H\|_F^2 &= \|\dot{\mathbf{A}} - \dot{\mathbf{Q}}_1 \dot{\mathbf{Q}}_1^H \dot{\mathbf{M}} \dot{\mathbf{Q}}_2 \dot{\mathbf{Q}}_2^H + \dot{\mathbf{Q}}_1 \dot{\mathbf{Q}}_1^H \dot{\mathbf{M}} \dot{\mathbf{Q}}_2 \dot{\mathbf{Q}}_2^H - \dot{\mathbf{Q}}_1 \dot{\mathbf{M}} \dot{\mathbf{Q}}_2^H\|_F^2 \\ &= \|\dot{\mathbf{A}} - \dot{\mathbf{Q}}_1 \dot{\mathbf{Q}}_1^H \dot{\mathbf{M}} \dot{\mathbf{Q}}_2 \dot{\mathbf{Q}}_2^H\|_F^2 + \|\dot{\mathbf{Q}}_1^H \dot{\mathbf{A}} \dot{\mathbf{Q}}_2 - \dot{\mathbf{M}}\|_F^2. \end{aligned} \quad (8)$$

As pointed out in [23], under the Frobenius norm, the truncated QSVD offers the best low-rank approximation of a quaternion matrix in a least-squares sense. Such that, the result in (6) holds.

Because $\dot{\mathbf{A}}_K$ is the best low-rank approximation to $\dot{\mathbf{A}}$, and $\dot{\mathbf{Q}}_1 \dot{\mathbf{M}}_K \dot{\mathbf{Q}}_2$ is the best restricted (within a subspace) low-rank restriction to $\dot{\mathbf{A}}$ with respect to Frobenius norm. This leads to the following result

$$\|\dot{\mathbf{A}} - \dot{\mathbf{A}}_K\|_F \leq \|\dot{\mathbf{A}} - \dot{\mathbf{Q}}_1 \dot{\mathbf{M}}_K \dot{\mathbf{Q}}_2\|_F \leq \|\dot{\mathbf{A}} - \dot{\mathbf{Q}}_1 \dot{\mathbf{Q}}_1^H \dot{\mathbf{A}}_K \dot{\mathbf{Q}}_2 \dot{\mathbf{Q}}_2^H\|_F. \quad (9)$$

The second relation holds because $\dot{\mathbf{Q}}_1 \dot{\mathbf{Q}}_1^H \dot{\mathbf{A}}_K \dot{\mathbf{Q}}_2 \dot{\mathbf{Q}}_2^H$ is an undistinguished restricted Frobenius norm approximation to $\dot{\mathbf{A}}$. Next, we prove (7) holds,

$$\begin{aligned} &\|\dot{\mathbf{A}} - \dot{\mathbf{Q}}_1 \dot{\mathbf{Q}}_1^H \dot{\mathbf{A}}_K \dot{\mathbf{Q}}_2 \dot{\mathbf{Q}}_2^H\|_F^2 \\ &= \|\dot{\mathbf{A}} - \dot{\mathbf{A}}_K \dot{\mathbf{Q}}_2 \dot{\mathbf{Q}}_2^H + \dot{\mathbf{A}}_K \dot{\mathbf{Q}}_2 \dot{\mathbf{Q}}_2^H - \dot{\mathbf{Q}}_1 \dot{\mathbf{Q}}_1^H \dot{\mathbf{A}}_K \dot{\mathbf{Q}}_2 \dot{\mathbf{Q}}_2^H\|_F^2 \\ &= \|\dot{\mathbf{A}} - \dot{\mathbf{A}}_K \dot{\mathbf{Q}}_2 \dot{\mathbf{Q}}_2^H\|_F^2 + \|\dot{\mathbf{A}}_K \dot{\mathbf{Q}}_2 \dot{\mathbf{Q}}_2^H - \dot{\mathbf{Q}}_1 \dot{\mathbf{Q}}_1^H \dot{\mathbf{A}}_K \dot{\mathbf{Q}}_2 \dot{\mathbf{Q}}_2^H\|_F^2 \\ &\quad + \Re[\text{tr}((\dot{\mathbf{A}} - \dot{\mathbf{A}}_K \dot{\mathbf{Q}}_2 \dot{\mathbf{Q}}_2^H)^H (\dot{\mathbf{A}}_K \dot{\mathbf{Q}}_2 \dot{\mathbf{Q}}_2^H - \dot{\mathbf{Q}}_1 \dot{\mathbf{Q}}_1^H \dot{\mathbf{A}}_K \dot{\mathbf{Q}}_2 \dot{\mathbf{Q}}_2^H))], \end{aligned} \quad (10)$$

where the third term in the right side of the equation is equal to $\Re[\text{tr}((\dot{\mathbf{A}} - \dot{\mathbf{A}}_K \dot{\mathbf{Q}}_2 \dot{\mathbf{Q}}_2^H)^H (\mathbf{I}_{M \times M} - \dot{\mathbf{Q}}_1 \dot{\mathbf{Q}}_1^H) (\dot{\mathbf{A}}_K \dot{\mathbf{Q}}_2 \dot{\mathbf{Q}}_2^H))] = \Re[\text{tr}((\mathbf{I}_{M \times M} - \dot{\mathbf{Q}}_1 \dot{\mathbf{Q}}_1^H) (\dot{\mathbf{A}} - \dot{\mathbf{A}}_K \dot{\mathbf{Q}}_2 \dot{\mathbf{Q}}_2^H)^H (\dot{\mathbf{A}}_K \dot{\mathbf{Q}}_2 \dot{\mathbf{Q}}_2^H))] = 0$.

Combining (9) and (10), then we have

$$\begin{aligned}
& \|\dot{\mathbf{A}} - \dot{\mathbf{Q}}_1 \dot{\mathbf{M}}_K \dot{\mathbf{Q}}_2^H\|_F \\
& \leq \|\dot{\mathbf{A}} - \dot{\mathbf{A}}_K \dot{\mathbf{Q}}_2 \dot{\mathbf{Q}}_2^H\|_F + \|\dot{\mathbf{A}}_K \dot{\mathbf{Q}}_2 \dot{\mathbf{Q}}_2^H - \dot{\mathbf{Q}}_1 \dot{\mathbf{Q}}_1^H \dot{\mathbf{A}}_K \dot{\mathbf{Q}}_2 \dot{\mathbf{Q}}_2^H\|_F \\
& = \|\dot{\mathbf{A}} - \dot{\mathbf{A}}_K + \dot{\mathbf{A}}_K - \dot{\mathbf{A}}_K \dot{\mathbf{Q}}_2 \dot{\mathbf{Q}}_2^H\|_F + \|\dot{\mathbf{A}}_K \dot{\mathbf{Q}}_2 \dot{\mathbf{Q}}_2^H - \dot{\mathbf{Q}}_1 \dot{\mathbf{Q}}_1^H \dot{\mathbf{A}}_K \dot{\mathbf{Q}}_2 \dot{\mathbf{Q}}_2^H\|_F \\
& \leq \|\dot{\mathbf{A}} - \dot{\mathbf{A}}_K\|_F + \|\dot{\mathbf{A}}_K - \dot{\mathbf{A}}_K \dot{\mathbf{Q}}_2 \dot{\mathbf{Q}}_2^H\|_F + \|\dot{\mathbf{A}}_K \dot{\mathbf{Q}}_2 \dot{\mathbf{Q}}_2^H - \dot{\mathbf{Q}}_1 \dot{\mathbf{Q}}_1^H \dot{\mathbf{A}}_K \dot{\mathbf{Q}}_2 \dot{\mathbf{Q}}_2^H\|_F \\
& = \|\dot{\mathbf{A}} - \dot{\mathbf{A}}_K\|_F + \|\dot{\mathbf{A}}_K - \dot{\mathbf{A}}_K \dot{\mathbf{Q}}_2 \dot{\mathbf{Q}}_2^H\|_F + \|\dot{\mathbf{A}}_K - \dot{\mathbf{Q}}_1 \dot{\mathbf{Q}}_1^H \dot{\mathbf{A}}_K\|_F.
\end{aligned} \tag{11}$$

■

Basing on Algorithm 4, let $\hat{\mathbf{A}}_{CoR} = \dot{\mathbf{Q}}_1 \dot{\mathbf{M}}_K \dot{\mathbf{Q}}_2^H$ be the CoR-QURV low-rank approximation and $\dot{\mathbf{M}}_K$ be the best rank- K approximation of $\dot{\mathbf{M}}$, then we have $\|\dot{\mathbf{A}} - \hat{\mathbf{A}}_{CoR}\|_F \leq \|\dot{\mathbf{A}} - \dot{\mathbf{Q}}_1 \dot{\mathbf{M}}_K \dot{\mathbf{Q}}_2^H\|_F$. Then, we have $\|\dot{\mathbf{A}} - \hat{\mathbf{A}}_{CoR}\|_F \leq \|\dot{\mathbf{A}} - \dot{\mathbf{A}}_K\|_F + \|\dot{\mathbf{A}}_K - \dot{\mathbf{A}}_K \dot{\mathbf{Q}}_2 \dot{\mathbf{Q}}_2^H\|_F + \|\dot{\mathbf{A}}_K - \dot{\mathbf{Q}}_1 \dot{\mathbf{Q}}_1^H \dot{\mathbf{A}}_K\|_F$ holds.

Let $\dot{\mathbf{A}} \in \mathbb{H}^{M \times N}$, and $\dot{\mathbf{A}} = [\dot{\mathbf{U}}_K, \dot{\mathbf{U}}_0] \begin{bmatrix} \Sigma_K & \mathbf{0} \\ \mathbf{0} & \Sigma_0 \end{bmatrix} [\dot{\mathbf{V}}_K, \dot{\mathbf{V}}_0]^H$ is the QSVD of $\dot{\mathbf{A}}$, where $\dot{\mathbf{U}}_K \in \mathbb{H}^{M \times K}$, $\dot{\mathbf{U}}_0 \in \mathbb{H}^{M \times M-K}$ and $\dot{\mathbf{V}}_K \in \mathbb{H}^{N \times K}$, $\dot{\mathbf{V}}_0 \in \mathbb{H}^{N \times N-K}$ are column orthogonal, and $\Sigma_K \in \mathbb{R}^{K \times K}$, $\Sigma_0 = [\Sigma_2, \Sigma_3] \in \mathbb{R}^{M-K \times N-K}$ with $\Sigma_2 \in \mathbb{R}^{l-P-K \times l-P-K}$ and $\Sigma_3 \in \mathbb{R}^{M-l+P \times N-l+P}$. All Σ_i are real diagonal matrices, and $\sigma_k (k = 1, \dots, K)$ are singular values. Let P be an integer satisfies $2 \leq P + K \leq l$, we define $\tilde{\Omega} = \dot{\mathbf{V}}^H \dot{\Omega} = [\tilde{\Omega}_1^H, \tilde{\Omega}_2^H]^H \in \mathbb{H}^{N \times l}$, where $\tilde{\Omega}_1 \in \mathbb{H}^{l-P \times l}$ and $\tilde{\Omega}_2 \in \mathbb{H}^{N-l+P \times l}$. The upper bound of $\|\dot{\mathbf{A}} - \hat{\mathbf{A}}_{CoR}\|_F$ is hold in the quaternion domain, and can be summarized in the following theorem.

Theorem 5. *Assume that the quaternion matrix $\dot{\mathbf{A}}$ has a QSVD, as stated above, and that $2 \leq P + K \leq l$. The quaternion matrix $\hat{\mathbf{A}}_{CoR}$ is created using Algorithm 4. Given that $\tilde{\Omega}_1$ has a full row rank. Then*

$$\|\dot{\mathbf{A}} - \hat{\mathbf{A}}_{CoR}\|_F \leq \|\dot{\mathbf{A}}_0\|_F + \sqrt{\frac{\alpha^2 \|\tilde{\Omega}_2\|_2^2 \|\tilde{\Omega}_1^\dagger\|_2^2}{1 + \beta^2 \|\tilde{\Omega}_2\|_2^2 \|\tilde{\Omega}_1^\dagger\|_2^2}} + \sqrt{\frac{\eta^2 \|\tilde{\Omega}_2\|_2^2 \|\tilde{\Omega}_1^\dagger\|_2^2}{1 + \tau^2 \|\tilde{\Omega}_2\|_2^2 \|\tilde{\Omega}_1^\dagger\|_2^2}}, \tag{12}$$

where $\alpha = \sqrt{K} \frac{\sigma_{l-P+1}^2}{\sigma_K} (\frac{\sigma_{l-P+1}}{\sigma_K})^{2p}$, $\beta = \frac{\sigma_{l-P+1}^2}{\sigma_1 \sigma_K} (\frac{\sigma_{l-P+1}}{\sigma_K})^{2p}$, $\eta = \frac{\sigma_K}{\sigma_{l-P+1}} \alpha$, $\tau = \frac{1}{\sigma_{l-P+1}} \beta$.

Proof: Because the singular values of quaternion matrix are real, and the norm function also can be represented by the real counterpart as can be seen in the Appendix, the proof of Theorem 5 is similar to the proof of Theorem 5 in [21]. Likewise, we can construct two quaternion matrices as

$$\dot{\mathbf{W}} = (\Sigma_3^T \Sigma_3)^{p+1} \tilde{\mathbf{\Omega}}_2 \tilde{\mathbf{\Omega}}_1^\dagger \begin{pmatrix} \Sigma_K^{-2p-2} \\ \mathbf{0}_{l-P-K \times K} \end{pmatrix},$$

$$\dot{\mathbf{D}} = \Sigma_3 (\Sigma_3^T \Sigma_3)^p \tilde{\mathbf{\Omega}}_2 \tilde{\mathbf{\Omega}}_1^\dagger \begin{pmatrix} \Sigma_K^{-2p-1} \\ \mathbf{0}_{l-P-K \times K} \end{pmatrix}.$$

Besides,

$$\|\dot{\mathbf{A}}_K - \dot{\mathbf{Q}}_1 \dot{\mathbf{Q}}_1^H \dot{\mathbf{A}}_K\|_F \leq \frac{\sqrt{K} \|\dot{\mathbf{D}} \Sigma_1\|_2 \sigma_1}{\sqrt{\|\dot{\mathbf{D}} \Sigma_1\|_2^2 + \sigma_1^2}}, \quad (13)$$

$$\|\dot{\mathbf{A}}_K - \dot{\mathbf{A}}_K \dot{\mathbf{Q}}_2 \dot{\mathbf{Q}}_2^H\|_F \leq \frac{\sqrt{K} \|\dot{\mathbf{W}} \Sigma_1\|_2 \sigma_1}{\sqrt{\|\dot{\mathbf{W}} \Sigma_1\|_2^2 + \sigma_1^2}} \quad (14)$$

are also hold in the quaternion domain.

According to the definition of $\dot{\mathbf{W}}$, $\dot{\mathbf{D}}$, and the property of $\|\dot{\mathbf{A}}\|_2 = \|\dot{\mathbf{A}}_C\|_2$, where $\dot{\mathbf{A}}_C$ is the column representation of $\dot{\mathbf{A}}$. Then we have

$$\frac{\|\dot{\mathbf{W}} \Sigma_1\|_2}{\|\tilde{\mathbf{\Omega}}_2\|_2 \|\tilde{\mathbf{\Omega}}_1^\dagger\|_2} \leq \frac{\sigma_{l-P+1}^2}{\sigma_K} \left(\frac{\sigma_{l-P+1}}{\sigma_K}\right)^{2p}, \quad (15)$$

$$\frac{\|\dot{\mathbf{D}} \Sigma_1\|_2}{\|\tilde{\mathbf{\Omega}}_2\|_2 \|\tilde{\mathbf{\Omega}}_1^\dagger\|_2} \leq \sigma_{l-P+1} \left(\frac{\sigma_{l-P+1}}{\sigma_K}\right)^{2p}. \quad (16)$$

Because the real function $f(x) = \frac{x}{\sqrt{1+x^2}}$ is monotonically increasing and substituting (15) and (16) into (13) and (14), then the theorem holds. ■

Remark 5. Theorem 5 shows that the upper bound of $\|\dot{\mathbf{A}} - \dot{\mathbf{A}}_{CoR}\|_F$ mainly depends on the ratio $\frac{\sigma_{l-P+1}}{\sigma_K}$. The power approaches reduce the additional components in the error boundary by exponentially decreasing the aforementioned ratios. Therefore, as p increases, the components decrease rapidly, approaching zero in an exponential manner. Nevertheless, this leads to the increase of the computation cost.

Proposition 1. Let $\dot{\Omega} = \Omega_0 + \Omega_1 i + \Omega_2 j + \Omega_3 k \in \mathbb{H}^{M \times N}$, $M \leq N$, where Ω_i ($i = 0, 1, 2, 3$) are standard Gaussian matrices. For any $\alpha > 0$, we have $\mathbb{E} \left(\sqrt{\frac{\alpha^2 \|\dot{\Omega}\|_2^2}{1 + \beta^2 \|\dot{\Omega}\|_2^2}} \right) \leq \sqrt{\frac{\alpha^2 \nu^2}{1 + \beta^2 \nu^2}}$, where $\nu = 3(\sqrt{M} + \sqrt{N}) + 3$.

The proof is given in the Appendix.

Proposition 2. Let $\dot{\Omega} = \Omega_0 + \Omega_1 i + \Omega_2 j + \Omega_3 k \in \mathbb{H}^{M \times N}$, $M \leq N$, where Ω_i ($i = 0, 1, 2, 3$) are standard Gaussian matrices. For any $\alpha > 0$, we have $\mathbb{E} \left(\sqrt{\frac{\alpha^2 \|\dot{\Omega}^\dagger\|_2^2}{1 + \beta^2 \|\dot{\Omega}^\dagger\|_2^2}} \right) \leq \sqrt{\frac{\alpha^2 \nu^2}{1 + \beta^2 \nu^2}}$, where $\nu = \frac{e\sqrt{4N+2}}{p+1}$.

The proof is given in the Appendix.

Theorem 6. With the notation of Theorem 5, for Algorithm 4, we have

$$\mathbb{E} \|\dot{\mathbf{A}} - \hat{\mathbf{A}}_{CoR}\|_F \leq \|\dot{\mathbf{A}}_0\|_F + (1 + \gamma_K) \sqrt{K} \nu \sigma_{l-P+1} \gamma_K, \quad (17)$$

where $\nu = (3(\sqrt{N} + \sqrt{N}) + 3) \frac{e\sqrt{4N+2}}{P+1}$ and $\gamma_K = \frac{\sigma_{l-P+1}}{\sigma_K}$.

Proof: By utilizing Lemma 2 in [13], $\tilde{\Omega} = \dot{\mathbf{V}}^H \dot{\Omega} = [\tilde{\Omega}_1^H, \tilde{\Omega}_2^H]^H$ follows $N(0, 4I_N)$, where $\tilde{\Omega}_1 \in \mathbb{H}^{l-P \times l}$ and $\tilde{\Omega}_2 \in \mathbb{H}^{N-l+P \times l}$ are disjoint submatrices. So we first take expectations over $\tilde{\Omega}_2$ and next over $\tilde{\Omega}_1$. By invoking Theorem 5, Proposition 1, and Proposition 2, we have

$$\begin{aligned} & \mathbb{E} \|\dot{\mathbf{A}} - \hat{\mathbf{A}}_{CoR}\|_F \\ &= \|\dot{\mathbf{A}}_0\|_F + \mathbb{E}_{\tilde{\Omega}_1} \mathbb{E}_{\tilde{\Omega}_2} \left(\sqrt{\frac{\alpha^2 \|\tilde{\Omega}_2\|_2^2 \|\tilde{\Omega}_1^\dagger\|_2^2}{1 + \beta^2 \|\tilde{\Omega}_2\|_2^2 \|\tilde{\Omega}_1^\dagger\|_2^2}} + \sqrt{\frac{\eta^2 \|\tilde{\Omega}_2\|_2^2 \|\tilde{\Omega}_1^\dagger\|_2^2}{1 + \tau^2 \|\tilde{\Omega}_2\|_2^2 \|\tilde{\Omega}_1^\dagger\|_2^2}} \right) \\ &\leq \|\dot{\mathbf{A}}_0\|_F + \mathbb{E}_{\tilde{\Omega}_1} \left(\sqrt{\frac{\alpha^2 \nu_1^2 \|\tilde{\Omega}_1^\dagger\|_2^2}{1 + \beta^2 \nu_1^2 \|\tilde{\Omega}_1^\dagger\|_2^2}} + \sqrt{\frac{\eta^2 \nu_1^2 \|\tilde{\Omega}_1^\dagger\|_2^2}{1 + \tau^2 \nu_1^2 \|\tilde{\Omega}_1^\dagger\|_2^2}} \right) \\ &\leq \|\dot{\mathbf{A}}_0\|_F + \sqrt{\frac{\alpha^2 \nu_1^2 \nu_2^2}{1 + \beta^2 \nu_1^2 \nu_2^2}} + \sqrt{\frac{\eta^2 \nu_1^2 \nu_2^2}{1 + \tau^2 \nu_1^2 \nu_2^2}} \\ &\leq \|\dot{\mathbf{A}}_0\|_F + (\alpha + \eta) \nu_1 \nu_2, \end{aligned} \quad (18)$$

where $\alpha + \eta = (1 + \frac{1}{\gamma_K})\alpha = (1 + \frac{1}{\gamma_K})\sqrt{K}\gamma_K\sigma_{l-p+1} = (1 + \gamma_K)\sqrt{K}\sigma_{l-p+1}$. So we have $\mathbb{E}\|\dot{\mathbf{A}} - \hat{\mathbf{A}}_{CoR}\|_F \leq \|\dot{\mathbf{A}}_0\|_F + (1 + \gamma_K)\sqrt{K}\sigma_{l-p+1}\nu_1\nu_2$, where $\nu_1 = 3(\sqrt{M} + \sqrt{N}) + 3$ and $\nu_2 = \frac{e\sqrt{4N+2}}{p+1}$. \blacksquare

Similarly, we give the theoretical analysis for quaternion tensor cases and take third-order quaternion tensor as an example. The linearly invertible transformation we adopted is QDCT, and the corresponding invertible transformation is Inverse Quaternion Discrete Cosine Transform (IQDCT). The QDCT process and IQDCT process is denoted as $\mathcal{D}(\cdot)$ and $\mathcal{ID}(\cdot)$, respectively. Firstly, basing on Algorithm 5, supposing that quaternion tensor data $\dot{\mathbf{A}} \in \mathbb{H}^{I_1 \times I_2 \times I_3}$, let $\hat{\mathbf{A}} = \mathcal{D}(\dot{\mathbf{A}})$, $\dot{\mathbf{Q}}_1^k \in \mathbb{H}^{I_1 \times l}$, and $\dot{\mathbf{Q}}_2^k \in \mathbb{H}^{I_2 \times l}$ ($k = 1 \cdots I_3$). Let $\hat{\mathbf{Q}}_1(:, :, k) = \dot{\mathbf{Q}}_1^k$ and $\hat{\mathbf{Q}}_2(:, :, k) = \dot{\mathbf{Q}}_2^k$. Then we have the following theorem.

Theorem 7. *Let $\hat{\mathbf{Q}}_1 \in \mathbb{H}^{I_1 \times l \times I_3}$, $\hat{\mathbf{Q}}_2 \in \mathbb{H}^{I_2 \times l \times I_3}$ be quaternion matrices constructed by Algorithm 5. Let $\hat{\mathbf{M}}_K(:, :, k)$ be the best rank- K approximation of $\hat{\mathbf{Q}}_1(:, :, k)^H \hat{\mathbf{A}}(:, :, k) \hat{\mathbf{Q}}_2(:, :, k) \in \mathbb{H}^{l \times l}$. Let $\dot{\mathbf{Q}}_1 = \mathcal{ID}(\hat{\mathbf{Q}}_1)$, $\dot{\mathbf{Q}}_2 = \mathcal{ID}(\hat{\mathbf{Q}}_2)$, and $\dot{\mathbf{M}}_K = \mathcal{ID}(\hat{\mathbf{M}}_K)$. Then, $\dot{\mathbf{M}}_K$ is an optimal solution of the following optimization problem:*

$$\min_{\dot{\mathbf{M}}, \text{rank}(\dot{\mathbf{M}}) \leq k} \|\dot{\mathbf{A}} - \dot{\mathbf{Q}}_1 \star_{QT} \dot{\mathbf{M}} \star_{QT} \dot{\mathbf{Q}}_2^H\|_F = \|\dot{\mathbf{A}} - \dot{\mathbf{Q}}_1 \star_{QT} \dot{\mathbf{M}}_K \star_{QT} \dot{\mathbf{Q}}_2^H\|_F, \quad (19)$$

besides, the rank of each $\dot{\mathbf{M}}(:, :, k)$ is small than or equal to K . Moreover,

$$\begin{aligned} \|\dot{\mathbf{A}} - \dot{\mathbf{Q}}_1 \star_{QT} \dot{\mathbf{M}}_K \star_{QT} \dot{\mathbf{Q}}_2^H\|_F &\leq \|\dot{\mathbf{A}} - \dot{\mathbf{A}}_K\|_F + \|\dot{\mathbf{A}}_K - \dot{\mathbf{Q}}_1 \star_{QT} \dot{\mathbf{Q}}_1^H \star_{QT} \dot{\mathbf{A}}_K\|_F \\ &\quad + \|\dot{\mathbf{A}}_K - \dot{\mathbf{A}}_K \star_{QT} \dot{\mathbf{Q}}_2 \star_{QT} \dot{\mathbf{Q}}_2^H\|_F. \end{aligned} \quad (20)$$

Lemma 1. *Let $\dot{\mathbf{A}}_{CoR} = \dot{\mathbf{U}} \star_{QT} \dot{\mathbf{T}} \star_{QT} \dot{\mathbf{V}}^H$ as obtained in Algorithm 5. Then we have $\|\dot{\mathbf{A}} - \dot{\mathbf{A}}_{CoR}\|_F \leq \|\dot{\mathbf{A}} - \dot{\mathbf{Q}}_1 \star_{QT} \dot{\mathbf{M}}_K \star_{QT} \dot{\mathbf{Q}}_2^H\|_F$.*

Proof: Let $\hat{\mathbf{A}}_{CoR} = \mathcal{D}(\dot{\mathbf{A}})$. Basing on Algorithm 5, the k th frontal slice of $\hat{\mathbf{A}}_{CoR}(:, :, k) = \dot{\mathbf{Q}}_1^{kH} \hat{\mathbf{A}}(:, :, k) \dot{\mathbf{Q}}_2^k$. Utilizing the definition \star_{QT} in [15] and the unitary property in QDCT, then we have $\|\dot{\mathbf{A}} - \dot{\mathbf{A}}_{CoR}\|_F^2 = \sum_{k=1}^{I_3} \|\hat{\mathbf{A}}(:, :, k) - \dot{\mathbf{Q}}_1^k \dot{\mathbf{M}}^k \dot{\mathbf{Q}}_2^{kH}\|_F^2$. Denoting $\dot{\mathbf{M}}_K^k$ as the best rank- K approximation of

$\dot{\mathbf{M}}^k$, then $\|\hat{\mathcal{A}}(:, :, k) - \dot{\mathcal{Q}}_1^k \dot{\mathbf{M}}^k \dot{\mathcal{Q}}_2^{kH}\|_F \leq \|\hat{\mathcal{A}}(:, :, k) - \dot{\mathcal{Q}}_1^k \dot{\mathbf{M}}_K^k \dot{\mathcal{Q}}_2^{kH}\|_F$, which completes the proof. \blacksquare

Let $\dot{\mathcal{A}} \in \mathbb{H}^{I_1 \times I_1 \times I_3}$ and $\hat{\mathcal{A}} = \mathcal{D}(\dot{\mathcal{A}})$. For every frontal slice of $\hat{\mathcal{A}}$, we have $\hat{\mathcal{A}}(:, :, k) = [\dot{\mathbf{U}}_K^k, \dot{\mathbf{U}}_0^k] \begin{bmatrix} \Sigma_K^k & \mathbf{0} \\ \mathbf{0} & \Sigma_0^k \end{bmatrix} [\dot{\mathbf{V}}_K^k, \dot{\mathbf{V}}_0^k]^H$ is the QSVD of $\hat{\mathcal{A}}(:, :, k)$, where $\hat{\mathcal{U}}_K(:, :, k) = \dot{\mathbf{U}}_K^k \in \mathbb{H}^{I_1 \times K}$, $\hat{\mathcal{U}}_0(:, :, k) = \dot{\mathbf{U}}_0^k \in \mathbb{H}^{I_1 \times I_1 - K}$ and $\hat{\mathcal{V}}_K(:, :, k) = \dot{\mathbf{V}}_K^k \in \mathbb{H}^{I_2 \times K}$, $\hat{\mathcal{V}}_0(:, :, k) = \dot{\mathbf{V}}_0^k \in \mathbb{H}^{I_2 \times I_2 - K}$ are column orthogonal, and $\hat{\mathcal{S}}_K(:, :, k) = \Sigma_K^k \in \mathbb{R}^{K \times K}$, $\hat{\mathcal{S}}_0(:, :, k) = \Sigma_0^k \in \mathbb{R}^{I_1 - K \times I_2 - K}$ are real diagonal matrices, and σ_i^k ($i = 1, \dots, K$) are singular values. Let P be an integer satisfies $2 \leq P + K \leq l$, we define $\tilde{\mathcal{Q}}^k = \dot{\mathbf{V}}^{kH} \dot{\mathcal{Q}} = [\tilde{\mathcal{Q}}_1^{kH}, \tilde{\mathcal{Q}}_2^{kH}]^H \in \mathbb{H}^{I_2 \times l}$, where $\tilde{\mathcal{Q}}_1^k \in \mathbb{H}^{l-P \times l}$ and $\tilde{\mathcal{Q}}_2^k \in \mathbb{H}^{(I_2-l+P) \times l}$. Basing on the Theorem 5 for quaternion matrix cases, the upper bound of $\|\dot{\mathcal{A}} - \dot{\mathcal{A}}_{CoR}\|_F$ is also hold, and can be summarized in the following theorem.

Theorem 8. *Assuming that the quaternion tensor $\dot{\mathcal{A}}$ has a TQt-SVD as defined in Theorem 2, and the the corresponding QSVD in the transformed domain are summarized in the above with $2 \leq P + K \leq l$. $\dot{\mathcal{A}}_{CoR}$ is quaternion tensor constructed by Algorithm 5. Assuming $\tilde{\mathcal{Q}}_1^k$ is full row rank. Then*

$$\|\dot{\mathcal{A}} - \dot{\mathcal{A}}_{CoR}\|_F \leq \|\dot{\mathcal{A}}_0\|_F + \sum_{k=1}^{I_3} \sqrt{\frac{\alpha_k^2 \|\tilde{\mathcal{Q}}_2^k\|_2^2 \|\tilde{\mathcal{Q}}_1^{k\dagger}\|_2^2}{1 + \beta_k^2 \|\tilde{\mathcal{Q}}_2^k\|_2^2 \|\tilde{\mathcal{Q}}_1^{k\dagger}\|_2^2}} + \sqrt{\frac{\eta_k^2 \|\tilde{\mathcal{Q}}_2^k\|_2^2 \|\tilde{\mathcal{Q}}_1^{k\dagger}\|_2^2}{1 + \tau_k^2 \|\tilde{\mathcal{Q}}_2^k\|_2^2 \|\tilde{\mathcal{Q}}_1^{k\dagger}\|_2^2}}, \quad (21)$$

where $\alpha_k = \sqrt{K} \frac{\sigma_{l-P+1}^{k2}}{\sigma_K^k} (\frac{\sigma_{l-P+1}^k}{\sigma_K^k})^{2p}$, $\beta_k = \frac{\sigma_{l-P+1}^{k2}}{\sigma_1^k \sigma_K^k} (\frac{\sigma_{l-P+1}^k}{\sigma_K^k})^{2p}$, $\eta = \frac{\sigma_K}{\sigma_{l-P+1}^k} \alpha_k$, $\tau_k = \frac{1}{\sigma_{l-P+1}^k} \beta_k$.

Theorem 9. *With the notation of Theorem 7, for Algorithm 5 we have*

$$\mathbb{E} \|\dot{\mathcal{A}} - \dot{\mathcal{A}}_{CoR}\|_F \leq \|\dot{\mathcal{A}}_0\|_F + \frac{\sqrt{K} \nu}{I_3} \sum_{k=1}^{I_3} (1 + \gamma_K^k) \sigma_{l-P+1}^k \gamma_K^k, \quad (22)$$

where $\nu = (3(\sqrt{N} + \sqrt{N}) + 3) \frac{e\sqrt{4N+2}}{P+1}$ and $\gamma_K = \frac{\sigma_{l-P+1}^k}{\sigma_K^k}$.

Basing on the above analysis, proof of the quaternion matrix case, and the proof of Theorem 4.1-4.3 in [26] for the real tensor cases, the proof of Theorem 7-9 are similar, so we omit the specific process here.

6. Experimental Results

In this section, the efficiency of the proposed algorithms are tested. The accuracy and the corresponding time computation are assessed for the approximation of QURV and CoR-QURV by applying them to some simulated low-rank quaternion matrices and real color images. Similarly, the QTURV and CoR-QTURV are tested by applying them to simulated low-rank quaternion tensors and real color videos. All the experiments were implemented in MATLAB R2019a, on a PC with a 3.00GHz CPU and 8GB RAM. The Quaternion Toolbox for Matlab¹ and the Tensor Toolbox for Matlab² are also adopted in the following experiment.

6.1. Settings

Each color image is represented by a pure quaternion matrix as $\dot{\mathbf{O}} = \mathbf{O}_R i + \mathbf{O}_G j + \mathbf{O}_B k \in \mathbb{H}^{M \times N}$, where \mathbf{O}_R , \mathbf{O}_G , and \mathbf{O}_B are RGB channels' pixel values separately. A color video is presented as a pure quaternion tensor $\dot{\mathcal{O}} = \mathcal{O}_R i + \mathcal{O}_G j + \mathcal{O}_B k \in \mathbb{H}^{M \times N \times f}$, where $M \times N$ is the size of each frame of the video, f is the number of frames, and \mathcal{O}_R , \mathcal{O}_G , and \mathcal{O}_B are the pixel values of RGB channels separately. For a given quaternion matrix rank $K < \min(M, N)$, the best rank-K approximation is $\dot{\mathbf{A}}_{URV,K} = \dot{\mathbf{U}}_K \dot{\mathbf{R}}_K \dot{\mathbf{V}}_K^H$, where $\dot{\mathbf{U}}_K = \dot{\mathbf{U}}(:, 1 : K)$, $\dot{\mathbf{V}}_K = \dot{\mathbf{V}}$, and $\dot{\mathbf{R}}_K = \dot{\mathbf{R}}(1 : K, :)$ with $\dot{\mathbf{U}}$, $\dot{\mathbf{V}}$, and $\dot{\mathbf{R}}$ are derived from Algorithm 1 or Algorithm 4. For a given quaternion tensor, the best TQt-rank-K approximation is $\dot{\mathcal{A}}_{URV,K} = \dot{\mathcal{U}}_K \star_{QT} \dot{\mathcal{R}}_K \star_{QT} \dot{\mathcal{V}}_K^H$, where $\dot{\mathcal{U}}_K = \dot{\mathcal{U}}(:, 1 : K, :)$, $\dot{\mathcal{V}}_K = \dot{\mathcal{V}}$, and $\dot{\mathcal{R}}_K = \dot{\mathcal{R}}(1 : K, :, :)$ with $\dot{\mathcal{U}}$, $\dot{\mathcal{V}}$, and $\dot{\mathcal{R}}$ are derived from Algorithm 3 or Algorithm 5.

The running time is tested by the pair ‘‘tic-toc’’ (in seconds). The Relative Error (RE) are defined as $\frac{\|\dot{\mathbf{A}} - \dot{\mathbf{A}}_{Rec}\|_F}{\|\dot{\mathbf{A}}\|_F}$, where $\dot{\mathbf{A}}_{Rec}$ is the recovered result of $\dot{\mathbf{A}}$ and $\frac{\|\dot{\mathcal{A}} - \dot{\mathcal{A}}_{Rec}\|_F}{\|\dot{\mathcal{A}}\|_F}$, where $\dot{\mathcal{A}}_{Rec}$ is the recovered result of $\dot{\mathcal{A}}$.

6.2. Testing the proposed QURV and CoR-QURV algorithms

In this section, synthetic quaternion matrices and several color images are used to test the efficiency of the proposed QURV and CoR-QURV. The truncated-QSVD is approximated by $\dot{\mathbf{U}}(:, 1 : K) \dot{\mathbf{R}}(1 : K, 1 : K) \dot{\mathbf{V}}(:, 1 : K)^H$, where $\dot{\mathbf{U}}$, $\dot{\mathbf{S}}$ and, $\dot{\mathbf{V}}$ are obtained by QSVD. The truncated-QQRC

¹<https://qtfm.sourceforge.io>

²<http://www.tensortoolbox.org>

is approximated by $\dot{\mathbf{Q}}(:, 1 : K)(\dot{\mathbf{R}}\dot{\mathbf{P}}^T)(1 : K, :)$, where $\dot{\mathbf{Q}}$, $\dot{\mathbf{R}}$, and $\dot{\mathbf{P}}$ are obtained by QQRCP.

Example 6.1. Consider a quaternion matrix $\dot{\mathbf{A}}$ is specified in the following format

$$\dot{\mathbf{A}} = \dot{\mathbf{P}}\dot{\mathbf{Q}}^H, \quad (23)$$

where $\dot{\mathbf{P}} \in \mathbb{H}^{500 \times 100}$ and $\dot{\mathbf{Q}} \in \mathbb{H}^{500 \times 100}$ are two random quaternion matrices created by “randq(·)” in Matlab.

Let the truncated number $K = 10 : 10 : 100$, the comparison of these three methods are displayed in Figure 1. It is observed from Figure 1 that regarding the RE, truncated QSVD outperforms truncated QURV and truncated QQRCP. Truncated QQRCP performs the worst in terms of RE. In terms of the running time, truncated QQRCP is the most time-saving method, followed by the truncated QURV method, while the truncated QSVD is the least efficient.

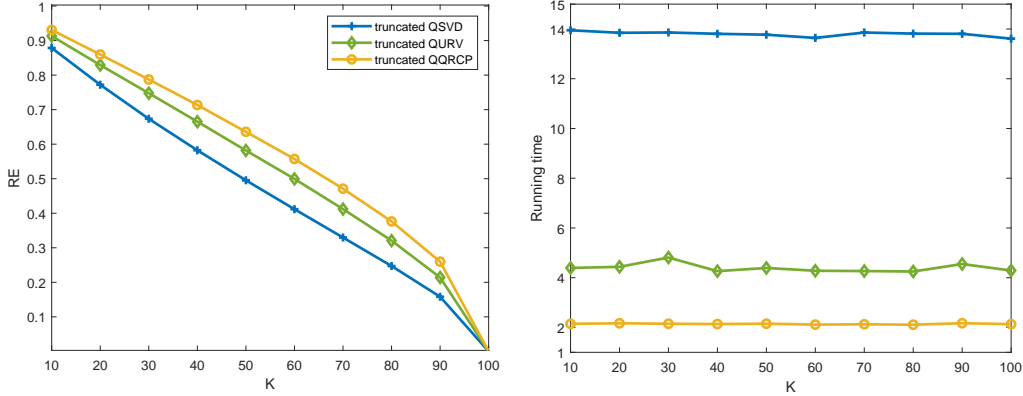


Figure 1: Comparison of the RE and running time of implementing truncated-QURV, truncated-QSVD, and truncated-QQRCP to Example 6.1 with $K = 10, 20, \dots, 100$.

Example 6.2. Consider a quaternion matrix $\dot{\mathbf{A}}$ is specified in the following format

$$\dot{\mathbf{A}} = \dot{\mathbf{U}}\dot{\mathbf{\Sigma}}\dot{\mathbf{V}}^H, \quad (24)$$

where $\dot{\mathbf{U}} \in \mathbb{H}^{500 \times 500}$ and $\dot{\mathbf{V}} \in \mathbb{H}^{500 \times 500}$ are two unitary quaternion matrices derived from computing QSVD of a random quaternion matrix $\bar{\mathbf{A}} \in \mathbb{H}^{500 \times 500}$. $\dot{\mathbf{\Sigma}}$ is a real diagonal matrix with the i th diagonal element is $1/i^2$ ($\dot{\mathbf{\Sigma}} = \text{diag}(1, 1/2^2, 1/3^2, \dots, 1/500^2)$).

Let $K = 2 : 2 : 20$, the comparison of these three methods are displayed in Figure 2. It is observed from Figure 2 that truncated QQRCP exhibits the

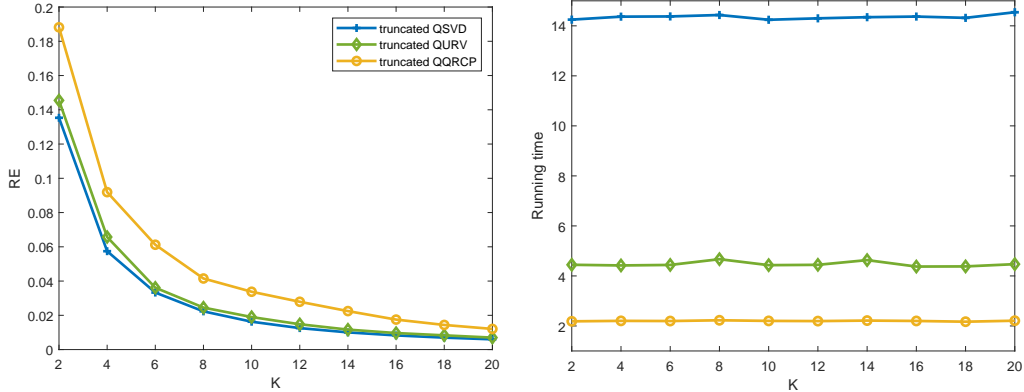


Figure 2: Comparison of the RE and running time of implementing truncated-QURV, truncated-QSVD, and truncated-QQRCP to Example 6.2 with $K = 2, 4, \dots, 20$.

worse performance in terms of RE, especially when the truncated number K is small. QSVD and QURV are comparable regarding the RE. In terms of the running time, truncated QQRCP saves the greatest time, followed by truncated QURV and truncated QSVD.

Then the comparison of randomized strategy is given by utilizing CoR-QURV and randQSVD to color images with the power parameter $p = 0, 1, 2$.

Example 6.3. Consider two color image as test images (can be seen in Figure 3). The size of “Flower” is 500×500 and the size of “House” is 1024×764 . The quaternion matrix representation for color image is given in subsection 6.1.

For image “Flower”, let $K = 20 : 20 : 200$, the comparison of CoR-QURV and randQSVD are displayed in Figure 4.

For image “House”, let $K = 40 : 40 : 400$, the comparison of CoR-QURV and randQSVD are displayed in Figure 5.

Observing from Figure 4-5, as the truncated number increases in size, the RE decreases and becomes more stable. As the truncated number increases in size, the techniques require more time to compute. Besides, Figure 4-5 also demonstrate that the CoR-QURV exhibits slightly lower performance in term of RE compared to randQSVD when they utilize the same power parameter p . When $p = 0$, the RE are more unfavorable compared to when $p = 1, 2$.



Figure 3: The test images: “Flower” and “House”.

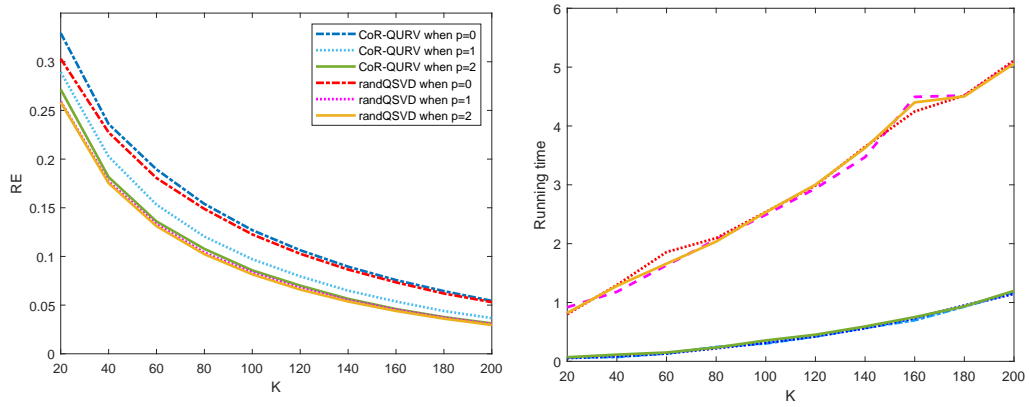


Figure 4: Comparison of the RE and running time of implementing CoR-QURV and randQSVD to Example 6.3 with $K = 20, 40, \dots, 200$.

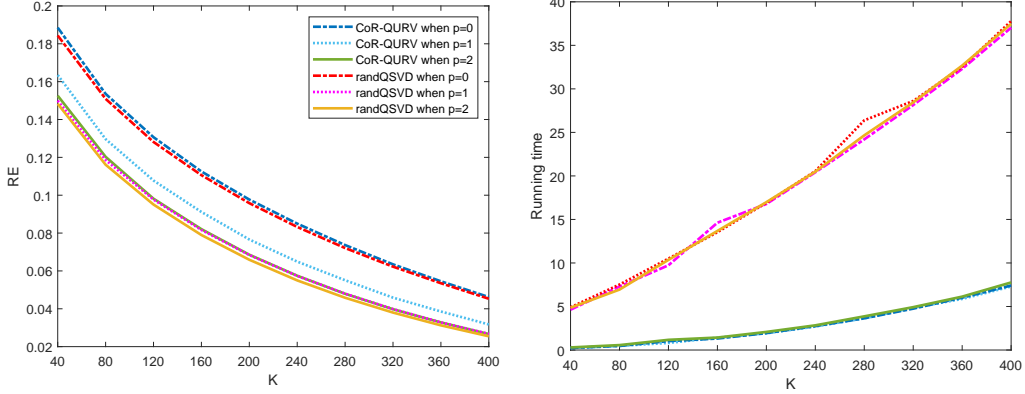


Figure 5: Comparison of the RE and running time of implementing CoR-QURV and randQSVD to Example 6.3 with $K = 40, 80, \dots, 400$.

When the value of p is equal to 2, the RE can achieve the optimal outcome for randQSVD and CoR-QURV. CoR-QURV outperforms randQSVD in term of running time for all values of p .

Next, the visual results of image “House” are shown in Figure 6. In this experiment, the power parameter $p = 1$, and the rank- K ($K = 20, 40, 400$) approximation of randQSVD is given in the first column. Meanwhile, the second column is the recovery of CoR-QURV. Observing from visual results in Figure 6, there is minimal distinction between visual impact of the original image and the recovered image when $K = 400$. When the truncated number is tiny, both CoR-QTURV and randQTSVD algorithms can approximately restore the original image, and there is not much visual difference between them.

6.3. Testing the proposed QTURV and CoR-QTURV algorithms

In this section, synthetic quaternion tensors and several color videos are used to test the efficiency of the proposed QTURV and CoR-QTURV. The TQt-rank- K approximation of truncated-QTSVD is approximated by $\dot{\mathcal{U}}(:, 1 : K, :) \star_{QT} \dot{\mathcal{R}}_K(1 : K, 1 : K, :) \star_{QT} \dot{\mathcal{V}}_K(:, 1 : K, :)^H$, where $\dot{\mathcal{U}}$, $\dot{\mathcal{S}}$ and, $\dot{\mathcal{V}}$ are obtained by QTSVD.

Example 6.4. Consider a quaternion matrix $\dot{\mathcal{A}}$ is specified in the following format

$$\dot{\mathcal{A}} = \dot{\mathcal{P}} \star_{QT} \dot{\mathcal{Q}}^H, \quad (25)$$



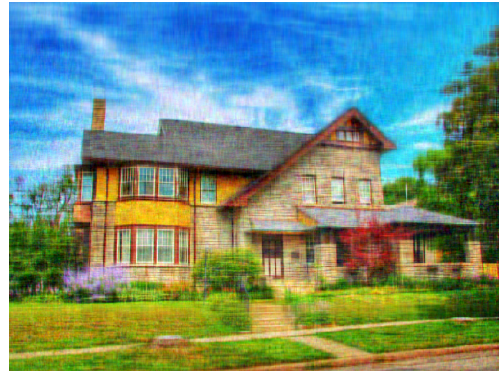
(a) randQSVD $K = 20$



(b) CoR-QURV $K = 20$



(c) randQSVD $K = 40$



(d) CoR-QURV $K = 40$



(e) randQSVD $K = 400$



(f) CoR-QURV $K = 400$

Figure 6: The rank- K approximation of “House” by utilizing CoR-QTURV and randQTSVD

where $\dot{\mathcal{P}} \in \mathbb{H}^{300 \times 20 \times 100}$ and $\dot{\mathcal{Q}} \in \mathbb{H}^{300 \times 20 \times 100}$ are two random quaternion tensors created by “randq(·)” in Matlab.

The TQt-rank is set to $K = 1 : 20$. The comparison between QTURV and QTSVD is shown in Figure 7. Figure 7 demonstrates that truncated QTSVD performs better than truncated QTURV in terms of the RE. Truncated QTURV is more time-efficient than truncated QTSVD.

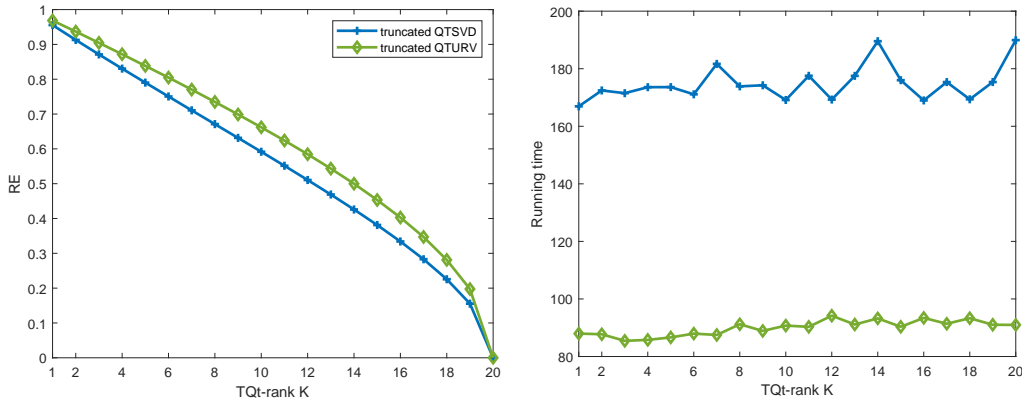


Figure 7: Comparison of the RE and running time of implementing truncated-QTSVD and truncated-QTURV to Example 6.4 with TQt-rank $K = 1, 2, \dots, 20$.

Example 6.5. Consider a quaternion tensor $\dot{\mathcal{A}}$ is specified in the following format

$$\dot{\mathcal{A}} = \dot{\mathcal{U}} \star_{QT} \mathcal{D} \star_{QT} \dot{\mathcal{V}}^H, \quad (26)$$

where $\dot{\mathcal{U}} \in \mathbb{H}^{300 \times 300 \times 30}$ and $\dot{\mathcal{V}} \in \mathbb{H}^{300 \times 300 \times 30}$ are two unitary quaternion tensors derived from computing QTSVD of a random quaternion matrix $\bar{\mathbf{A}} \in \mathbb{H}^{300 \times 300 \times 30}$. \mathcal{D} is a real diagonal tensor that is stacked by diagonal matrices with the i th diagonal element is $1/i^2$ ($\mathcal{D}(:, :, k) = \text{diag}(1, 1/2^2, 1/3^2, \dots, 1/300^2)$), $k = 1 : 30$.

Let the TQt-rank $K = 1 : 20$, the comparison of QTURV with QTSVD are displayed in Figure 8. Figure 8 illustrates that the truncated QTSVD method outperforms the truncated QTURV method in term of the RE. As the TQt-rank increases, the discrepancy in RE between truncated QTSVD and truncated QTURV is diminishing. In addition, the truncated QTURV

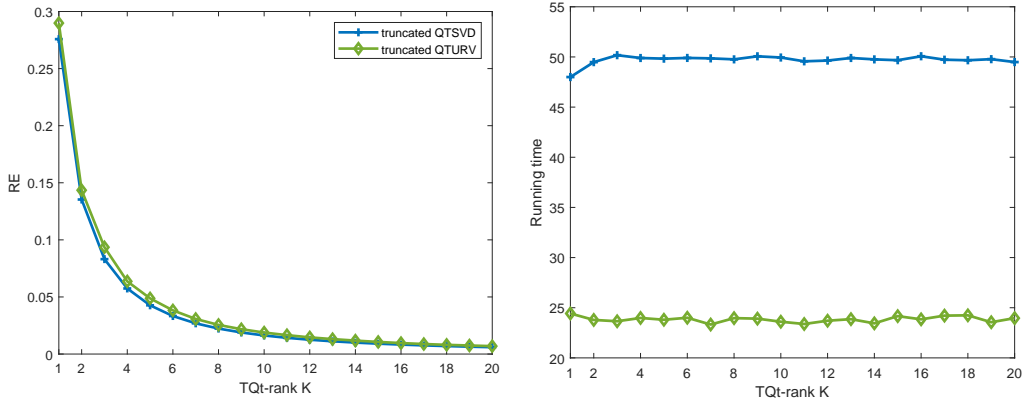


Figure 8: Comparison of the RE and running time of implementing truncated-QTSVD and truncated-QTURV to Example 6.5 with TQt-rank $K = 1, 2, \dots, 20$.

method is more time-efficient than the truncated QTSVD method in all situations.

Then the comparison of randomized strategy is given by utilizing CoR-QTURV and randQTSVD to color videos with the power parameter $p = 0, 1, 2$.

Example 6.6. Consider two color videos as test data (can be seen in Figure 9). The size of “Football” is $288 \times 352 \times 125$ and the size of “Landscape” is $288 \times 352 \times 250$. The quaternion tensor representation for color video is given in subsection 6.1.

For video “Football”, let the TQt-rank $K = 6 : 6 : 60$, the comparison of CoR-QTURV and randQTSVD is displayed in Figure 10.

For video “Landscape”, let the TQt-rank $K = 10 : 10 : 150$, the comparison of CoR-QTURV and randQTSVD is displayed in Figure 11.

The RE decreases as the TQt-rank increases, as observed in Figure 10-11. The techniques necessitate an increased amount of computation time as the TQt-rank increases. Additionally, the CoR-QTURV exhibits slightly inferior performance in terms of RE compared to randQTSVD when the same power parameter p is used, as illustrated in Figure 10-11. The RE are more poor when $p = 0$ than when $p = 1, 2$. The RE can accomplish the optimal outcome for randQTSVD and CoR-QTURV when the value of p is equal to 2. For all values of p , CoR-QTURV outperforms randQTSVD in terms of running time.



Figure 9: The test videos: “Football” and “Landscape”.

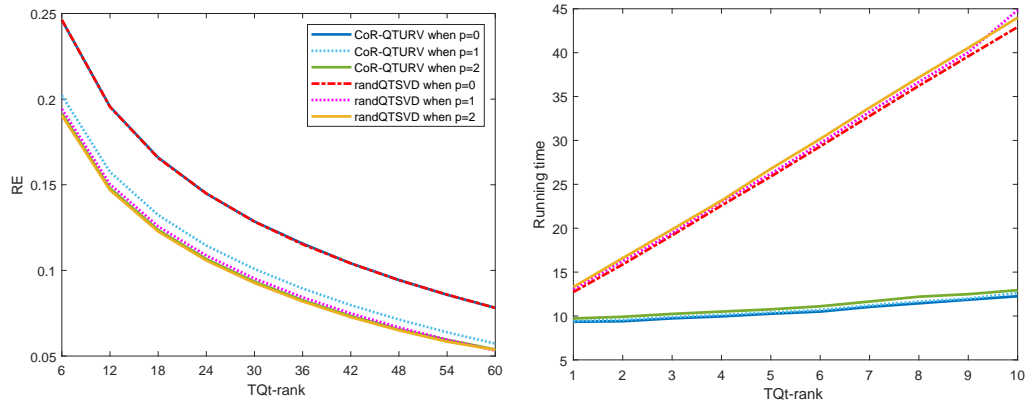


Figure 10: Comparison of the RE and running time of implementing CoR-QTURV and randQTSVD to Example 6.6 with TQt-rank $K = 6, 12, \dots, 60$.

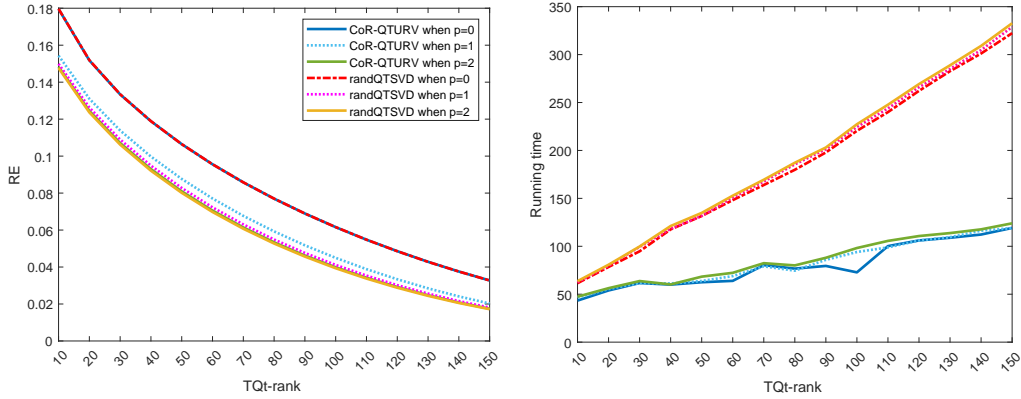


Figure 11: Comparison of the RE and running time of implementing CoR-QTURV and randQTSVD to Example 6.6 with TQt-rank $K = 10, 20, \dots, 150$.

Next, the visual results of video “Football” are shown in Figure 12 (the results of the first frame) and Figure 13 (the results of the last frame). In this experiment, the power parameter $p = 1$, and the TQt-rank $K = 6, 12, 18, 36$. The first column is the original frame, the second column is the recovery of randQTSVD, and the last column is the recovery of CoR-QTURV.

The numbers on jerseys in the frame are roughly visible, and the visual impact of the original frame and the recovered frame is minimal when $K = 36$, as evidenced by the visual results in Figure 12-13. The original video can be approximately restored by both CoR-QTURV and randQTSVD algorithms when the TQt-rank is small, and there is not a significant visual difference between them.

7. Conclusion

This paper proposes a novel decomposition for quaternion matrix and quaternion tensor. Firstly, the definition of QTUTV is provided, followed by the definition of this decomposition for quaternion tensor. In order to enhance the efficiency of the algorithms, a randomized technique is employed, resulting in the development of the CoR-QURV and CoR-QTURV. The error bound analysis is presented for randomized approaches. Finally, the experiment conducted on synthetic data, color images, and color videos provides evidence of the effectiveness of the proposed algorithms. Additionally, the developed quaternion-based decomposition can be used for the low-rank



Figure 12: The TQt-rank- K approximation results of “Football” (the first frame) by utilizing CoR-QTURV and randQTSVD



Figure 13: The TQt-rank-K approximation results of “Football” (the last frame) by utilizing CoR-QTURV and randQTSVD

quaternion tensor completion model or quaternion tensor robust component analysis problem. The quaternion-based UTV decomposition can be considered as an alternative to the truncated QSVD in certain problems.

Appendix A. Proof of Theorem 1

To prove Proposition 1, we first present several key results for using later on.

Proposition 3. [27] *Let h be a real valued Lipschitz function on matrices, then for all \mathbf{X}, \mathbf{Y} :*

$$|h(\mathbf{X}) - h(\mathbf{Y})| \leq L \|\mathbf{X} - \mathbf{Y}\|_F, \quad (\text{A.1})$$

where $L > 0$. For any $m \times n$ standard Gaussian matrix \mathbf{G} and $u > 0$, then $\mathbb{P}\{h(\mathbf{G}) \geq \mathbb{E}h(\mathbf{G}) + Lu\} \leq e^{-u^2/2}$.

Proposition 4. [13] *For $\dot{\mathbf{A}} = \mathbf{A}_0 + \mathbf{A}_1i + \mathbf{A}_2j + \mathbf{A}_3k \in \mathbb{H}^{M \times N}$, define the real counterpart and the column representation respectively as follows*

$$\gamma_{\dot{\mathbf{A}}} = \begin{bmatrix} \mathbf{A}_0 & -\mathbf{A}_1 & -\mathbf{A}_2 & -\mathbf{A}_3 \\ \mathbf{A}_1 & \mathbf{A}_0 & -\mathbf{A}_3 & \mathbf{A}_2 \\ \mathbf{A}_2 & \mathbf{A}_3 & \mathbf{A}_0 & -\mathbf{A}_1 \\ \mathbf{A}_3 & -\mathbf{A}_2 & \mathbf{A}_1 & \mathbf{A}_0 \end{bmatrix}, \quad \dot{\mathbf{A}}_C = \begin{bmatrix} \mathbf{A}_0 \\ \mathbf{A}_1 \\ \mathbf{A}_2 \\ \mathbf{A}_3 \end{bmatrix}.$$

Then $\|\dot{\mathbf{A}}\|_F = \frac{1}{2}\|\gamma_{\dot{\mathbf{A}}}\|_F$ and $\|\dot{\mathbf{A}}\|_2 = \|\dot{\mathbf{A}}_C\|_2$.

Proposition 5. *For $\dot{\mathbf{\Omega}} = \mathbf{\Omega}_0 + \mathbf{\Omega}_1i + \mathbf{\Omega}_2j + \mathbf{\Omega}_3k$, where $\mathbf{\Omega}_i, i = 0, 1, 2, 3$ are random and independently Gaussian random matrices. Define a function $h(\dot{\mathbf{\Omega}}) = \|\dot{\mathbf{\Omega}}\|_2$. Then by utilizing Lemma 6 in [13], we have $\mathbb{E}(h(\dot{\mathbf{\Omega}})) \leq 3(\sqrt{M} + \sqrt{N}) < 3(\sqrt{M} + \sqrt{N}) + 1 \triangleq \epsilon$.*

Proposition 6. [28] *Let $g(\cdot)$ be a nonnegative continuously differentiable function with $g(0) = 0$, and \mathbf{G} is a random matrix, then $\mathbb{E}_g(\mathbf{G}) = \int_0^\infty g'(x) \mathbb{P}\{\|\mathbf{G}\|_2 \geq x\} dx$.*

Proof of Proposition 1

Proof: Define $h(\dot{\mathbf{A}}_C) = \|\gamma_{\dot{\mathbf{A}}}\|_2 = \|[\mathbf{J}_0 \dot{\mathbf{A}}_C \ \mathbf{J}_1 \dot{\mathbf{A}}_C \ \mathbf{J}_2 \dot{\mathbf{A}}_C \ \mathbf{J}_3 \dot{\mathbf{A}}_C]\|_2$, where $\mathbf{J}_0 = \mathbf{I}_4 \otimes \mathbf{I}_M$, $\mathbf{J}_1 = [-\mathbf{e}_2 \ \mathbf{e}_1 \ \mathbf{e}_4 \ -\mathbf{e}_3] \otimes \mathbf{I}_M$, $\mathbf{J}_2 = [-\mathbf{e}_3 \ -\mathbf{e}_4 \ \mathbf{e}_1 \ \mathbf{e}_2] \otimes \mathbf{I}_M$, $\mathbf{J}_3 = [-\mathbf{e}_4 \ \mathbf{e}_3 \ -\mathbf{e}_2 \ \mathbf{e}_1] \otimes \mathbf{I}_M$, with \mathbf{e}_i be the i th column of \mathbf{I}_4 . Utilizing Proposition 3 and Proposition 4, we have $h(\dot{\mathbf{A}}_C - \dot{\mathbf{B}}_C) = |\|\gamma_{\dot{\mathbf{A}}}\|_2 - \|\gamma_{\dot{\mathbf{B}}}\|_2| =$

$\|\dot{\mathbf{A}}\|_2 - \|\dot{\mathbf{B}}\|_2 \leq \|\dot{\mathbf{A}} - \dot{\mathbf{B}}\|_2 \leq \|\dot{\mathbf{A}}_C - \dot{\mathbf{B}}_C\|_F$. That means that $h(\cdot)$ is a Lipschitz function. Next, utilizing Proposition 6 with Lipschitz constant $L = 1$, we have $\mathbb{P}\{\|\dot{\mathbf{G}}\|_2 \geq x\} \leq e^{-u^2/2}$, where $u = x - \epsilon$. Then, we first define the real function $g(x) \triangleq \sqrt{\frac{\alpha^2 x^2}{1 + \beta^2 x^2}}$ with $g'(x) = \frac{\alpha^2 x^2}{(1 + \beta^2 x^2)^2 \sqrt{\frac{\alpha^2 x^2}{1 + \beta^2 x^2}}}$, where $\alpha > 0, \beta > 0$.

Then we have

$$\begin{aligned}
\mathbb{E} \left(\sqrt{\frac{\alpha^2 \|\dot{\mathbf{\Omega}}\|_2^2}{1 + \beta^2 \|\dot{\mathbf{\Omega}}\|_2^2}} \right) &= \mathbb{E} \left(\sqrt{\frac{\alpha^2 \|\dot{\mathbf{\Omega}}_C\|_2^2}{1 + \beta^2 \|\dot{\mathbf{\Omega}}_C\|_2^2}} \right) \\
&= \int_0^\infty g'(x) \mathbb{P}\{\|\dot{\mathbf{\Omega}}\|_2 \geq x\} dx \\
&\leq \sqrt{\frac{\alpha^2 \epsilon^2}{1 + \beta^2 \epsilon^2}} + \int_\epsilon^\infty \frac{\alpha^2 x^2}{(1 + \beta^2 x^2)^2 \sqrt{\frac{\alpha^2 x^2}{1 + \beta^2 x^2}}} e^{-\frac{(x-\epsilon)^2}{2}} dx \\
&\leq \sqrt{\frac{\alpha^2 \epsilon^2}{1 + \beta^2 \epsilon^2}} + \frac{\alpha^2}{(1 + \beta^2 \epsilon^2)^2 \sqrt{\frac{\alpha^2 \epsilon^2}{1 + \beta^2 \epsilon^2}}} \int_0^\infty (u + \epsilon) e^{-\frac{u^2}{2}} du \\
&= \sqrt{\frac{\alpha^2 \epsilon^2}{1 + \beta^2 \epsilon^2}} + \frac{\alpha^2}{(1 + \beta^2 \epsilon^2)^2 \sqrt{\frac{\alpha^2 \epsilon^2}{1 + \beta^2 \epsilon^2}}} (1 + \epsilon \sqrt{\frac{\pi}{2}}).
\end{aligned} \tag{A.2}$$

Comparing the inequality in Proposition 1 with (A.2), we need to find a constant $v > 0$ such that

$$\sqrt{\frac{\alpha^2 \epsilon^2}{1 + \beta^2 \epsilon^2}} + \frac{\alpha^2}{(1 + \beta^2 \epsilon^2)^2 \sqrt{\frac{\alpha^2 \epsilon^2}{1 + \beta^2 \epsilon^2}}} (1 + \epsilon \sqrt{\frac{\pi}{2}}) \leq \sqrt{\frac{\alpha^2 v^2}{1 + \beta^2 v^2}}, \tag{A.3}$$

which leads to $v^2 - \epsilon^2 \geq (\epsilon \sqrt{\frac{\pi}{2}} + 1) \frac{1 + \beta^2 v^2}{1 + \beta^2 \epsilon^2} \left[\sqrt{\frac{\alpha^2 \epsilon^2}{1 + \beta^2 \epsilon^2}} + 1 \right]$.

The right side of the inequality approaches maximum value as $\beta \rightarrow \infty$. Thus $v^2 - \epsilon^2 \geq \frac{2\epsilon^2}{\epsilon^2} (\epsilon \sqrt{\frac{\pi}{2}} + 1)$, which solves to $v \geq \frac{\epsilon^2}{\sqrt{\epsilon^2 - 2(\epsilon \sqrt{\frac{\pi}{2}} + 1)}}$. Because the defined $\epsilon \geq 7$, the inequality holds when $v = 3(\sqrt{M} + \sqrt{N}) + 4 = \epsilon + 3$. ■

Appendix B. Proof of Proposition 2

Proof: Based on the Theorem 7 in [13], we have $\mathbb{P}\{\|\dot{\mathbf{G}}^\dagger\|_2 \geq x\} \leq$

$\bar{c}x^{-2(2N-2M+2)}$, where $\bar{c} = \frac{c'}{4^{2N-2M+2}}$ and $c' = \frac{\pi^{-3}}{4(N-M+1)(2N-2M+3)} \cdot \left[\frac{e\sqrt{4N+2}}{2N-2M+2} \right]^{2(2N-2M+2)}$.

Following a similar track in the proof of Proposition 1, we have

$$\begin{aligned}
\mathbb{E} \left(\sqrt{\frac{\alpha^2 \|\dot{\mathbf{\Omega}}^\dagger\|_2^2}{1 + \beta^2 \|\dot{\mathbf{\Omega}}^\dagger\|_2^2}} \right) &= \mathbb{E} \left(\sqrt{\frac{\alpha^2 \|\dot{\mathbf{\Omega}}_C^\dagger\|_2^2}{1 + \beta^2 \|\dot{\mathbf{\Omega}}_C^\dagger\|_2^2}} \right) \\
&= \int_0^\infty g'(x) \mathbb{P}\{\|\dot{\mathbf{\Omega}}^\dagger\|_2 \geq x\} dx \\
&\leq \sqrt{\frac{\alpha^2 c^2}{1 + \beta^2 c^2}} + \int_c^\infty \frac{\alpha^2 x^2}{(1 + \beta^2 x^2)^2 \sqrt{\frac{\alpha^2 x^2}{1 + \beta^2 x^2}}} \bar{c} x^{-2(2N-2M+2)} dx \\
&\leq \sqrt{\frac{\alpha^2 c^2}{1 + \beta^2 c^2}} + \frac{\alpha^2 \bar{c}}{(1 + \beta^2 c^2)^2 \sqrt{\frac{\alpha^2 c^2}{1 + \beta^2 c^2}}} \int_c^\infty x^{-4(N-M+1)+1} dx \\
&= \sqrt{\frac{\alpha^2 c^2}{1 + \beta^2 c^2}} + \frac{\alpha^2 \bar{c}}{(1 + \beta^2 c^2)^2 \sqrt{\frac{\alpha^2 c^2}{1 + \beta^2 c^2}}} \cdot \frac{c^{-4(N-M+1)+2}}{4(N-M+1)-2}.
\end{aligned} \tag{B.1}$$

Let $N - M = q \geq 0$, then we need to find a $v > 0$ such that $\sqrt{\frac{\alpha^2 c^2}{1 + \beta^2 c^2}} + \frac{\alpha^2 \bar{c}}{(1 + \beta^2 c^2)^2 \sqrt{\frac{\alpha^2 c^2}{1 + \beta^2 c^2}}} \cdot \frac{c^{-4(q+1)}}{4(q+1)-2} \leq \sqrt{\frac{\alpha^2 v^2}{1 + \beta^2 v^2}}$. This equation is similar to equation (A.3), with difference being the coefficients in the second term on the left side. Thus, its solution similarly satisfies $v \geq \frac{c^2}{\sqrt{c^2 - \frac{2\bar{c}c^2 c^{-4(q+1)}}{4(q+1)-2}}}$. Next, substituting the value of \bar{c} to the right side of the inequality, we have $v \geq \frac{c}{\sqrt{1 - \frac{\pi^{-3}}{4(q+1)(2q+1)(2q+3)} \left(\frac{4(q+1)}{e\sqrt{4n+2}} c \right)^{-4(q+1)}}}$. The value $v = \frac{e\sqrt{4N+2}}{q+1}$ satisfies this inequality for $c = \frac{e\sqrt{4N+2}}{4(q+1)} \left(\frac{\pi^{-3}}{4(2q+1)(q+1)} \right)^{\frac{1}{4(q+1)}}$. ■

References

- [1] Sir William Rowan Hamilton LL.D. P.R.I.A. F.R.A.S. Hon. M. R. Soc. Ed. and Dub. Hon. or Corr. M. II. on quaternions; or on a new system of imaginaries in algebra. *Philosophical Magazine Series 3*, 25(163):10–13, 1844.

- [2] Konstantinos Daniilidis and Eduardo Bayro-Corrochano. The dual quaternion approach to hand-eye calibration. In *13th International Conference on Pattern Recognition, ICPR 1996, Vienna, Austria, 25-19 August, 1996*, pages 318–322. IEEE Computer Society, 1996.
- [3] Hao Liu, Xiafu Wang, and Yisheng Zhong. Quaternion-based robust attitude control for uncertain robotic quadrotors. *IEEE Trans. Ind. Informatics*, 11(2):406–415, 2015.
- [4] Eduardo Bayro-Corrochano, Sven Buchholz, and Gerald Sommer. Self-organizing clifford neural network. In *Proceedings of International Conference on Neural Networks (ICNN'96), Washington, DC, USA, June 3-6, 1996*, pages 120–125. IEEE, 1996.
- [5] Jifei Miao, Kit Ian Kou, and Wankai Liu. Low-rank quaternion tensor completion for recovering color videos and images. *Pattern Recognit.*, 107:107505, 2020.
- [6] Yifen Ke, Changfeng Ma, Zhigang Jia, Yajun Xie, and Riwei Liao. Quasi non-negative quaternion matrix factorization with application to color face recognition. *J. Sci. Comput.*, 95(2):38, 2023.
- [7] Mingcui Zhang, Wenxv Ding, Ying Li, Jianhua Sun, and Zhihong Liu. Color image watermarking based on a fast structure-preserving algorithm of quaternion singular value decomposition. *Signal Process.*, 208:108971, 2023.
- [8] Chaoyan Huang, Zhi Li, Yubing Liu, Tingting Wu, and Tiejong Zeng. Quaternion-based weighted nuclear norm minimization for color image restoration. *Pattern Recognit.*, 128:108665, 2022.
- [9] Yongyong Chen, Xiaolin Xiao, and Yicong Zhou. Low-rank quaternion approximation for color image processing. *IEEE Trans. Image Process.*, 29:1426–1439, 2020.
- [10] Jifei Miao and Kit Ian Kou. Quaternion-based bilinear factor matrix norm minimization for color image inpainting. *IEEE Trans. Signal Process.*, 68:5617–5631, 2020.

- [11] Yong Chen, Zhi-Gang Jia, Yan Peng, Yaxin Peng, and Dan Zhang. A new structure-preserving quaternion QR decomposition method for color image blind watermarking. *Signal Process.*, 185:108088, 2021.
- [12] Minghui Wang and Wenhao Ma. A structure-preserving method for the quaternion LU decomposition in quaternionic quantum theory. *Comput. Phys. Commun.*, 184(9):2182–2186, 2013.
- [13] Qiaohua Liu, Sitao Ling, and Zhigang Jia. Randomized quaternion singular value decomposition for low-rank matrix approximation. *SIAM J. Sci. Comput.*, 44(2):870, 2022.
- [14] Huan Ren, Ru-Ru Ma, Qiaohua Liu, and Zheng-Jian Bai. Randomized quaternion QLP decomposition for low-rank approximation. *J. Sci. Comput.*, 92(3):80, 2022.
- [15] Jifei Miao and Kit Ian Kou. Quaternion tensor singular value decomposition using a flexible transform-based approach. *Signal Process.*, 206:108910, 2023.
- [16] Quaternion tensor train rank minimization with sparse regularization in a transformed domain for quaternion tensor completion. *Knowledge-Based Systems*, 284:111222, 2024.
- [17] G. W. Stewart. An updating algorithm for subspace tracking. *IEEE Trans. Signal Process.*, 40(6):1535–1541, 1992.
- [18] G. W. Stewart. Updating a rank-revealing ULV decomposition. *SIAM J. Matrix Anal. Appl.*, 14(2):494–499, 1993.
- [19] Ricardo D. Fierro and Per Christian Hansen. Low-rank revealing UTV decompositions. *Numer. Algorithms*, 15(1):37–55, 1997.
- [20] G. W. Stewart. The QLP approximation to the singular value decomposition. *SIAM J. Sci. Comput.*, 20(4):1336–1348, 1999.
- [21] Maboud Farzaneh Kaloorazi and Rodrigo C. de Lamare. Subspace-orbit randomized decomposition for low-rank matrix approximations. *IEEE Trans. Signal Process.*, 66(16):4409–4424, 2018.
- [22] Fuzhen Zhang. Quaternions and matrices of quaternions. *Linear Algebra Appl.*, 251:21–57, 1997.

- [23] Carl Eckart and Gale Young. The approximation of one matrix by another of lower rank. *Psychometrika*, 1(3):211–218, 1936.
- [24] Eckhard Hitzer. Quaternion fourier transform on quaternion fields and generalizations. *CoRR*, abs/1306.1023, 2013.
- [25] Mawardi Bahri, Eckhard S. M. Hitzer, Akihisa Hayashi, and Ryuichi Ashino. An uncertainty principle for quaternion fourier transform. *Comput. Math. Appl.*, 56(9):2398–2410, 2008.
- [26] Maolin Che and Yimin Wei. An efficient algorithm for computing the approximate t-urv and its applications. *J. Sci. Comput.*, 92(3):93, 2022.
- [27] Nathan Halko, Per-Gunnar Martinsson, and Joel A. Tropp. Finding structure with randomness: Probabilistic algorithms for constructing approximate matrix decompositions. *SIAM Rev.*, 53(2):217–288, 2011.
- [28] Ming Gu. Subspace iteration randomization and singular value problems. *SIAM J. Sci. Comput.*, 37(3), 2015.